Published in final edited form as:
Cancer Discov. 2013 February ; 3(2): 182–197. doi:10.1158/2159-8290.CD-12-0292.

Senescence sensitivity of breast cancer cells is defined by positive feedback loop between CIP2A and E2F1

Anni Laine[1,2,3], **Harri Sihto**[4], **Christophe Come**[1], **Mathias T. Rosenfeldt**[5], **Aleksandra Zwolinska**[6], **Minna Niemelä**[1,7], **Anchit Khanna**[8], **Edward K. Chan**[9], **Veli-Matti Kähäri**[10], **Pirkko-Liisa Kellokumpu-Lehtinen**[11], **Owen J. Sansom**[5], **Gerard I. Evan**[12], **Melissa R. Junttila**[12], **Kevin M. Ryan**[5], **Jean-Christophe Marine**[6], **Heikki Joensuu**[13], and **Jukka Westermarck**[1,2,*]

[1]Turku Centre for Biotechnology, University of Turku and Åbo Akademi University, Turku, Finland [2]Department of Pathology, University of Turku, Turku, Finland [3]Turku Doctoral Program of Biomedical Sciences, Turku, Finland [4]Laboratory of Molecular Oncology, Molecular Cancer Biology program, Biomedicum, University of Helsinki, Helsinki, Finland [5]The Beatson Institute for Cancer Research, Glasgow, G61 1BD, UK [6]Center for Human Genetics & VIB11 - Center for Biology of Disease, Laboratory for Molecular Cancer Biology, VIB-KULeuven, Leuven , Belgium [7]Department of Medical Biochemistry and Genetics, University of Turku, Turku, Finland [8]Institute of Biomedical Technology, University of Tampere and Tampere University Hospital, Tampere, Finland [9]Department of Oral Biology, University of Florida, 32610-0424 Gainesville, FL, USA [10]Department of Dermatology, University of Turku and Turku University Hospital, MediCity Research Laboratory, University of Turku, Turku, Finland [11]Department of Oncology, Tampere University Hospital and University of Tampere, Tampere, Finland [12]University of California San Francisco, Department of Pathology and Helen Diller Family Comprehensive Cancer Center, San Francisco, California 94143-0502, USA. [13]Department of Oncology, Helsinki University Central Hospital, and University of Helsinki, Helsinki, Finland

Abstract

Senescence induction contributes to cancer therapy responses and is crucial for p53-mediated tumor suppression. However, whether p53 inactivation actively suppresses senescence induction has been unclear. Here we demonstrate that E2F1 overexpression, due to p53 or p21 inactivation, promotes expression of human oncoprotein CIP2A, which in turn, by inhibiting PP2A activity, increases stabilizing serine 364 phosphorylation of E2F1. Several lines of evidence demonstrate that increased activity of E2F1-CIP2A feedback renders breast cancer cells resistant to senescence induction. Importantly, mammary tumorigenesis is impaired in a CIP2A deficient mouse model, and CIP2A deficient tumors display markers of senescence induction. Moreover, high CIP2A expression predicts for poor prognosis in a subgroup of breast cancer patients treated with senescence-inducing chemotherapy. Together these results implicate E2F1-CIP2A feedback loop

*Correspondence: jukwes@utu.fi.
Present addresses: Department of Biochemistry, Tennis Court Road, University of Cambridge, Cambridge CB2 1GA, UK (G.I.E.) Department of Molecular Biology, Genentech. Inc. South San Francisco, CA 94080, USA (M.R.J.) Lowy Cancer Research Centre C25, University of New South Wales, Sydney, NSW 2052, Australia (A.K) Biotech Research and Innovation Centre, University of Copenhagen, DK-2200 Copenhagen N, Denmark (C.C).

Authors declare that they have no competing financial interests.

SUPPLEMENTAL DATA The Supplemental Data includes 5 supplementary figures with legends, 3 supplementary tables and supplementary materials and methods, including sequences of siRNAS, RT-PCR primers and ChIP primers (Supplementary Table S3). This data can be found with this article online.

Europe PMC Funders Author Manuscripts

as a key determinant of breast cancer cell sensitivity to senescence induction. It also constitutes a promising pro-senescence target for therapy of cancers with inactivated p53-p21 pathway.

Introduction

Cellular senescence functions as a barrier that normal cells have to overcome in order to transform into cancer cells (1). Accordingly, analysis of several types of premalignant tumors, most notably benign skin nevi, has revealed the existence of senescent pretumorigenic cells (1, 2). The functional relevance of spontaneous senescence induction in preventing tumor initiation and progression has been demonstrated by several recent mouse studies (3-5).

Notably, although traditionally considered as apoptosis-inducing agents, most of the currently used chemotherapies exert their therapeutic effect at least partly by senescence induction (6, 7). Similarly, there is accumulating evidence that despite of the essential role of tumor suppressor p53 in mediating apoptosis induction by genotoxic stimuli and chemotherapies, its *in vivo* tumor suppressor activity is not dependent on apoptosis, but senescence induction (8-11). However, p53 function is inactivated in the majority of human cancers, and p53 inactivation correlates with poor patient survival in several cancer types including breast cancer (12). Traditionally, resistance of p53 mutant cells to chemotherapy has been linked to defective checkpoint function of p53 (13). However, we cannot exclude the possibility that in addition to defective checkpoint activity, p53 inhibition actively promotes mechanism(s) that confers cancer cells general resistance to chemotherapy-induced senescence. In addition to mutations, p53 is known to be inactivated in cancer cells by enhanced proteolytic degradation driven by ubiquitin ligases Mdm2 and MdmX (14). Although therapeutic strategies to activate senescence via inhibition of Mdm2/MdmX-p53 interactions have been under intense research lately (14), due to p53 mutations, they are unlikely to be efficient in large fraction of human tumors. Therefore, there is an urgent need to identify novel mechanisms that promote senescence resistance and tumor progression downstream of inactivated p53. Identification of such mechanisms would not only provide novel insights into senescence regulation, but could also facilitate development of novel pro-senescence therapy strategies for cancers harbouring inactivated p53 (6, 7).

E2F1 is an oncogenic transcription factor that is overexpressed in various human cancer types (15). Recent studies have indicated that E2F1's classical function in transcriptional activation of S phase-associated genes only partially explains its oncogenic activity (15, 16). Its transcriptional activity is negatively regulated by p53 through p21-mediated regulation of retinoblastoma (Rb) protein phosphorylation (15, 16), but expression and activity of E2F1 is also regulated directly by phosphorylation, independently of Rb (16, 17). p53 reactivation by small molecular activator Nutlin-3 inhibits protein expression of E2F1 and induces senescence-like growth arrest (18). Accordingly, knock-down of E2F1 expression also induces cellular senescence in p53-deficient cancer cells and blocks tumor growth (19-21). However, the mechanisms by which E2F1 prevents senescence induction in p53-deficient cells are currently unclear.

A human oncoprotein Cancerous Inhibitor of PP2A (CIP2A) is overexpressed in 65-90% of the patient tissue in almost all human cancer types studied thus far, and its expression correlates with cancer progression in a large variety of human malignancies (Table S1) (22-25). Even though CIP2A protein expression correlates with proliferation in human cancers (22-25), expression of CIP2A is not regulated by cell cycle activity (24). Overexpressed CIP2A transforms immortalized cells of either human or mouse origin (23, 26), whereas its depletion by RNAi inhibits anchorage independent growth of several types

Europe PMC Funders Author Manuscripts

of tumor cells (22-26). CIP2A's tumor promoting role has been demonstrated by several xenograft studies (22, 23, 25, 26), but the genetic evidence that it contributes to tumor progression is yet lacking. CIP2A's oncogenic function has been mostly linked to its capacity to prevent proteolytic degradation of MYC by promoting its serine 62 phosphorylation (23, 24, 27, 28). As CIP2A overexpression is one of the most frequent alterations in human cancers (Table S1), identification of novel mechanisms that regulates CIP2A, and oncogenic targets that could explain its significant correlation with human cancer progression, would be of general interest.

Here we demonstrate that CIP2A is a direct transcriptional target of E2F1 and that CIP2A overexpression increases expression of E2F1, phosphorylated at serine 364. The positive feedback loop between these two human oncoproteins is stimulated by p53 inactivation, and is critical for inhibition of senescence induction in human breast cancer cells. Moreover, our results strongly indicate that the E2F1-CIP2A positive feedback loop plays a role in the resistance towards senescence-inducing chemotherapy in human breast cancer patients. Furthermore, we provide the first genetic evidence for CIP2A's role in promoting breast cancer progression. Our data also indicates that this newly identified oncogenic mechanism is a potential pro-senescence target for therapy of cancers with inactivated p53.

Results

CIP2A expression is associated with p53 expression and adverse prognostic factors in human breast cancer

High CIP2A mRNA expression positively correlates with the presence of *p53* mutation in human breast cancer samples (22). In order to confirm that p53 inactivation in breast cancer cells correlates with CIP2A protein expression, a series of unselected human breast cancers were stained for CIP2A and p53 protein expression, by using a p53 antibody that we have recently shown to be indicative of p53 mutation (29). Out of the 1228 cancers investigated 46% were positive for CIP2A (Figure S1A,B), and CIP2A expression significantly correlated with high p53 immunopositivity (Figure 1A,B). However, despite statistical correlation between high p53 immunopositivity and increased CIP2A protein expression (Figure 1B), this analysis identified tumors in which CIP2A was highly expressed even in the absence of p53 immunopositivity. It is possible that in these cases CIP2A overexpression is due to high expression of MYC or ETS1 transcription factors, both shown recently to stimulate CIP2A expression in human cancer cells (24, 30). Moreover, CIP2A expression correlated significantly with several markers of aggressive disease such as a high KI-67 proliferation index, a large tumor size and a low histological grade of differentiation (Figure 1B and Figure S1C,D).

Wild-type p53 downregulates CIP2A expression

To study whether wild-type p53 negatively regulates CIP2A expression, p53 expression was inhibited by siRNA in cultured mouse embryonic fibroblasts (MEFs), and CIP2A expression was subsequently studied by western blotting. As shown in Figure 1C, inhibition of p53 expression in MEFs by two different siRNA sequences resulted in robust induction of CIP2A protein expression. Moreover, re-activation of wild-type p53 in MCF-7 human breast cancer cells with small-molecule inhibitors of Mdm2-p53 interaction, Nutlin-3 (31), or RITA (32), inhibited CIP2A expression both at mRNA and protein level (Figure 1D, E and Figure S2A,B). To confirm that CIP2A downregulation by Nutlin-3 is dependent on wild-type p53 function, we treated MDA-MB-231 human breast cancer cells, harbouring inactive mutant p53, with Nutlin-3. Nutlin-3 treatment had no effect on either p21 or CIP2A protein expression in MDA-MB-231 cells (Figure 1F). However, when wild-type p53 was introduced to these cells, CIP2A protein expression was inhibited in a concentration

dependent manner (Figure 1G). To further confirm that CIP2A expression is regulated by a p53-dependent mechanism, we treated isogenic wild-type and p53-/- HCT116 human colorectal cancer cells with p53-activating chemotherapy doxorubicin. In contrast to wild-type cells, p53-/- HCT116 cells were resistant to doxorubicin-induced inhibition of CIP2A mRNA expression (Figure 1H). In addition to in vitro models, we analyzed CIP2A expression in lymphoma tissue derived from a transgenic Eu-Myc mouse model carrying tamoxifen-inducible p53 (33). As shown in figures 1I and J, in vivo restoration of p53 function resulted in inhibition of CIP2A expression in lymphoma tissue, thus confirming that p53 negatively regulates oncoprotein CIP2A expression also *in vivo*. Interestingly, in addition to experimental data above, bioinformatic analysis of recently published CIP2A-regulated gene signature (34) with Ingenuity Transcription Factor Analysis software that reads transcription factor activities, demonstrated that transcriptional response to CIP2A knock-down mimicked most significantly the situation in which p53 is activated (Figure 1K and Table S2). These results together identify CIP2A as a novel *in vivo* target of wild-type p53 activity and indicate that p53-mediated CIP2A downregulation functionally contributes to p53 response.

E2F1 upregulates CIP2A expression downstream of inactivated p53

To study whether p53 regulates CIP2A expression at the transcriptional level, MCF-7 cells transfected with a *CIP2A* promoter luciferase construct containing the 1802bp upstream promoter fragment (30), were treated with Nutlin-3 or RITA. p53 reactivation by either of these compounds inhibited activity of *CIP2A* promoter but not the activity of the *egfr* promoter (35) that was used as a control (Figure 2A, S2C). Bioinformatic analysis of the −1802 fragment of *CIP2A* promoter revealed two putative p53 binding sites (Figure 2B, S2D). However, when a chromatin immunoprecipitation assay for p53 was performed in doxorubicin treated HCT-116 cells, we could not detect any enrichment for these two putative binding sites although p53 clearly accumulated on *mdm2* or *p21* promoters (Figure 2C). In support to these results, p53 was found not to bind to CIP2A promoter in chromatin immunoprecipitation sequencing (ChIP-Seq) analysis performed with control or Nutlin-3 treated MCF-7 cells (Data not shown (S. Aerts, personal communication)). These results indicate that although p53 activity inhibits *CIP2A* gene transcription, *CIP2A* is not a direct target gene of p53.

The p53 downstream target, p21, regulates gene expression by inhibiting cyclin dependent kinases (CDKs), which in turn leads to dephosphorylation of retinoblastoma protein (Rb), and consequent inhibition of an oncogenic transcription factor E2F1 (15, 16). We confirmed that Nutlin-3-induced CIP2A downregulation is associated with the activation of the above described p21 cascade, leading also to previously-observed inhibition of E2F1 protein expression (18)(Figure 2D). To study whether p21 induction is required for p53-mediated CIP2A downregulation, we used isogenic HCT-116 wild-type and p21-/- cells. In the unperturbed p21-/- cells, CIP2A expression was increased as compared to wild-type cells (Figure 2E). Interestingly, similar to p53-/- HCT-116 cells, p21-/- HCT-116 cells also were resistant to doxorubicin-induced CIP2A inhibition (Figure 2E). Moreover, p21 expression by adenoviral transduction inhibited E2F1 and CIP2A expression in MDA-MB-231 cells harboring mutated p53 (Figure 2F). Importantly, p21-elicited E2F1 inhibition was detected already at 24h timepoint (1d) and preceded downregulation of CIP2A protein expression (Figure 2F). These results suggest that increased E2F1 expression may stimulate CIP2A expression in cells with inactive p53 and p21. Supporting this hypothesis, CIP2A expression was inhibited in cells transfected with E2F1 targeting siRNA (Figure 2G). Importantly, CIP2A downregulation by E2F1 RNAi is unlikely to be caused by general inhibition of cell cycle activity, as CIP2A expression neither is sensitive to aphidicolin-elicited cell cycle arrest nor associated with by serum-induced cell cycle progression (24). Furthermore,

conditional tetracycline-induced overexpression of E2F1 resulted in CIP2A upregulation at the mRNA level (Figure 2H). To verify that CIP2A is a direct E2F1 target, we performed E2F1 chromatin immunoprecipitation in cells transfected with an E2F1 expression construct. E2F1 binding site at −378 to −361 in −1802 fragment of *CIP2A* promoter was predicted by using Genomatix-software. As shown in figure 2I, E2F1 antibody immunoprecipitation clearly enriched this putative *CIP2A* promoter E2F1 binding site from E2F1 overexpressing cells as compared to cells transfected with control vector or non-antibody controls. E2F1 binding to CIP2A promoter was further verified by ChIP-seq analysis from MCF-7 cells by using ENCODE database (Figure S2E).

Taken together, these results strongly imply down-regulation of CIP2A oncoprotein expression as a novel target mechanism for p53 tumor suppressor activity (Figure 2J). Moreover, these results demonstrate that E2F1 stimulates CIP2A expression in cells with inactive p53 and p21 (Figure 2J).

Inhibition of CIP2A expression is a prerequisite for p53-mediated senescence induction

In line with the indicated role for CIP2A as a p53 effector protein (Figure 1K), CIP2A depletion by RNAi in MCF-7 cells mimicked p53-activated senescence, as characterized by increased SA-beta-gal activity and flattened cell morphology in most of the cells (Figure 3A). Induction of senescence was verified in CIP2A siRNA transfected MCF-7 cells by increased expression of the p53-induced senescence marker decoy receptor 2 (DcR2)(11) (Figure 3B). Importantly, CIP2A depletion induced appearance of senescence phenotype also in p53 mutant MDA-MB-231 cells (Figure 3C), in which depletion of CIP2A causes long-term inhibition of xenograft tumor growth (22). Previously, we have shown that inhibition of CIP2A does not induce programmed cell death in HeLa cells (Junttila et al. 2007). As hypothesized, stable expression of CIP2A did not reverse obvious cell death phenotype in MCF-7 cells treated with RITA, a known inducer of p53-dependent cell death (Figure S2F,G, Issaeva et al. 2004). These results indicate that CIP2A downregulation is linked to p53-induced senescence.

In order to study whether CIP2A inhibition is truly required for p53-mediated senescence induction, Nutlin-3-induced CIP2A inhibition was prevented by infection of MCF-7 cells with CIP2A expressing adenovirus. Importantly, even though CIP2A overexpression did not prevent Nutlin-3-induced p21 induction (Figure 3D), it prevented senescence induction in MCF-7 cells. This was demonstrated by significant decrease in number of cells displaying SA-beta-gal activity and flattened cell morphology (Figure 3E and F), and inhibition of induction of several Nutlin-3-regulated genes that previously have been shown to be functionally involved in p53-induced senescence (36-38)(Figure 3G).

Overexpression of CIP2A was recently shown to induce resistance to cell proliferation inhibition in doxorubicin-treated MCF-7 cells (39). In line with doxorubicin-elicited inhibition of CIP2A mRNA expression in a p53- and p21-dependent manner (Figure 1I and 2E), also protein expression of both E2F1 and CIP2A was inhibited by doxorubicin treatment (Figure 3H). Importantly, as for Nutlin-3, stable expression of CIP2A rescued MCF-7 cells from doxorubicin-induced senescence (Figure 3I,J).

Positive feedback loop between CIP2A and E2F1 functions as a barrier for senescence induction

To investigate the underlying mechanism by which p53 reactivation-induced inhibition of CIP2A induces senescence, we studied the effect of CIP2A expression on Nutlin-3-induced p53-p21-p-Rb-E2F1 pathway function. As shown above (Figure 3D), stable expression of CIP2A did not affect Nutlin-3-induced p21 activation (Figure 4A). This suggests that the

mechanism through which CIP2A inhibits senescence may function downstream of p21. Moreover, p21-mediated CDK inhibition seemed to be intact in CIP2A overexpressing cells, since Rb dephosphorylation in Nutlin-3 treated cells was not affected (Figure 4A). However, stable expression of CIP2A did effectively prevent Nutlin-3-induced E2F1 protein downregulation (Figure 4A). Importantly, CIP2A seems to regulate E2F1 at the post-transcriptional level, as e2f1 mRNA was downregulated by Nutlin-3 in CIP2A adenovirus transduced cells at the same 8h timepoint (Figure 4B), at which E2F1 protein was inhibited only in control virus transduced cells (Figure 4A). E2F1 is known to negatively autoregulate its promoter activity followed by hypophosphorylation of Rb (40), and this most likely explains the downregulation of E2F1 at mRNA level by Nutlin-3. In support of post-translational effects of CIP2A on E2F1, CIP2A overexpression clearly increased expression of the serine-364 phosphorylated form of E2F1 (Figure 4C), previously shown to be relatively resistant to proteolytic degradation (17, 41). The stable nature of S364 phosphorylated E2F1 is further demonstrated by high levels of phospho-S364 E2F1 in Nutlin-3-treated, and CIP2A overexpressing cells at the 24h timepoint (Figure 4D). At this timepoint, expression of non-phosphorylated E2F1 was already inhibited, along with inhibition of *e2f1* mRNA expression (Figures 4E and data not shown). Slightly reduced expression of total E2F1 in CIP2A overexpressed cells (Figure 4A and C), suggests that CIP2A overexpression drives E2F1 protein to S364 phosphorylated form that may not be as readily detected by the total E2F1 antibody.

CIP2A inhibits phosphatase activity of serine/threonine phosphatase PP2A (23, 42). Furthermore, inhibition of two regulatory B subunits of PP2A, B55α and B56β, rescues CIP2A-depletion induced effects on colony growth and gene expression (34). Resulted to this, we hypothesized that PP2A holoenzymes consisting of either B55α or B56β subunits could be responsible for dephosphorylation of serine 364 residue of E2F1 in cancer cells. In fact, inhibition of B55α, but not B56β, resulted in increased phosphorylation of S364 E2F1 (Figure 4F, S3A). Moreover, similarly to CIP2A overexpression, depletion of B55α rescued E2F1 protein downregulation induced by Nutlin-3 (Figure 4G). Moreover, this effect was not observed with depletion of B56β (Figure 4G). Taken together, these results suggest that positive feedback mechanism from CIP2A to E2F1 is mediated by inhibition of PP2A complex containing B55α subunit.

Downregulation of E2F1 has been reported to induce senescence in a p53-independent manner and to prevent tumorigenesis (19-21). To demonstrate that loss of E2F1 results in induction of the senescent phenotype in the cell type studied, E2F1 expression was downregulated in MCF-7 cells by shRNA (shE2F1). E2F1 depletion significantly increased the number of SA-beta-gal positive cells as compared to control cells expressing non-targeted shRNA (ShNTC1) (Figure 4H,I). Moreover, E2F1 downregulation by either Nutlin-3, or by E2F1 shRNA, mirrored their effectiveness in inducing the senescent phenotype, but Nutlin-3 could not increase further SA-beta-gal positivity in E2F1 depleted cells (Figure 4H,I). These results indicate that E2F1 downregulation is critical for senescence induction by Nutlin-3-elicited p53 reactivation.

Recent studies have shown that cellular senescence can be triggered either by p21 induction or E2F1 inhibition also in cells carrying mutant p53 (4, 19, 20, 43). On the other hand, we show here that p21 overexpression downregulates E2F1 and CIP2A expression in p53-mutant MDA-MB-231 cells, in which CIP2A depletion provokes senescence induction (Figures 2F and 3C). To study whether CIP2A down regulation is required for senescence induced by p21, CIP2A adenovirus-infected MDA-MB-231 cells were re-infected with either control or p21-expressing adenovirus. As shown in figures 4J and K, stable expression of CIP2A rescued the senescence phenotype induced by p21 overexpression. Moreover, inhibition of Rb had no effect in CIP2A-depletion-induced senescence in MCF-7 cells

(Figure S3B,C), further indicating that CIP2A regulates senescence downstream of p53-p21-Rb pathway.

Taken together, these results uncover E2F1-CIP2A positive feedback loop and its role in determining cellular senescence induction in breast cancer cell lines. Interestingly, our results suggest that even transient stabilization of E2F1 upon p53 reactivation is sufficient to prevent initiation of senescence. Importantly, functional role of this newly identified feedback loop is not restricted to p53-induced senescence, but contributes also to senescence induction by p21 in p53 mutant cells.

CIP2A inactivation induces senescence and growth arrest, and restricts tumorigenesis in a breast cancer mouse model

We have recently generated a CIP2A hypomorphic mouse model ($CIP2A^{HOZ}$) using gene-trap technology (44). Despite efficient inhibition of CIP2A expression in all examined tissues, $CIP2A^{HOZ}$ mice do not show obvious developmental or growth defects (Figure S4A-G)(44). However, consistent with senescence phenotype observed in CIP2A depleted cancer cells (Figures 3A-C), MEFs isolated from $CIP2A^{HOZ}$ mouse embryos (Figure 5A) underwent growth arrest after only a few passages (Figure 5B), and displayed increased SA-beta-gal staining and flattened cell morphology (Figure 5C and D). Importantly, Nutlin-3 treatment of wild-type MEFs induced equal level of senescence as was observed in $CIP2A^{HOZ}$ cells spontaneously, but Nutlin-3 could not further increase senescence in $CIP2A^{HOZ}$ cells (Figure 5D). Moreover, overexpression of CIP2A rescued Nutlin-3 induced downregulation of E2F1 also in MEFs, indicating that CIP2A-mediated E2F1 stabilization is a conserved mechanism between humans and rodents (Figure 5E).

To study whether, in addition to p53 activation (10), also the loss of CIP2A suppresses tumorigenesis, we analyzed mammary tumor initiation and progression in MMTVneu breast cancer mouse model crossed with $CIP2A^{HOZ}$ mice. Notably, 35% of MMTVneu tumors are known to harbour mutations in the p53 DNA-binding domain, frequency relatively similar to that seen in unselected human breast cancer material (45). In accordance with results from human samples (22, 23), normal mouse mammary glands expressed very low levels of CIP2A (Figure 6A). However, CIP2A mRNA expression was greatly increased in MMTVneu x $CIP2A^{WT}$ (neu/WT) tumors (p=0,003)(Figure 6A), and efficient inhibition of CIP2A expression in MMTV-neu x $CIP2A^{HOZ}$ (neu/HOZ) tumors was confirmed by RT-PCR analysis (Figure 6A). Interestingly, as compared to neu/WT mice, neu/HOZ mice had less KI-67 positive epithelial cells in macroscopically tumor-free mammary glands (Figure 6B,C and Figure S4H). In line with these observations, the average number of mammary tumors per mice was significantly reduced in neu/HOZ mice (p=0,0220)(Figure 6D). Furthermore, follow-up of the tumors that developed in either of the genotypes demonstrated that the time for tumor growth from the day of tumor appearance to the day when the mice had to be sacrificed since the 20 mm maximum size of the largest tumor allowed was reached, was significantly delayed in neu/HOZ mice (p=0,0030)(Figure 6E).

In concert with *in vitro* results shown above, mammary tumors in CIP2A deficient mice displayed gene expression changes indicative of senescence induction (Figure 6F). Out of these senescence-inhibiting genes, down-regulated in neu/HOZ tumors (6, 7, 46-48), Twist1 and Id1 are particularly interesting, as they have both recently been shown to block oncogene-driven senescence in breast cancer cells (46, 48). Importantly, expression of p53-induced senescence marker DcR2 (11) was also increased in CIP2A deficient neu/HOZ tumors at the protein level (Figure 6H). Moreover, we observed spontaneous induction of SA-beta-gal expression in cultured cells isolated from neu/HOZ tumors (Figure 6G,H). Together, these results validate the senescence phenotype of CIP2A deficient breast cancer cells *in vivo.*

In order to confirm the *in vivo* role for CIP2A in inhibition of senescence in another setting, and without potentially confounding effects of mouse strain crossings, the effect of CIP2A expression in methylbenzanthracene (DMBA) treatment-induced senescence in mouse skin (5) was examined. As hypothesized, we detected significantly more SA-beta-gal staining in DMBA treated CIP2A^{HOZ} mouse skin as compared to wild type mouse skin (Figure S4I,J). Together, these results validate induction of senescence as a plausible cause for decreased mammary tumorigenesis in CIP2A deficient mice.

In order to examine whether above described role for CIP2A in promoting E2F1 expression would be observed also in *in vivo* setting, we performed western blot analysis from tumor lysates. Indeed, E2F1 expression was decreased in neu/HOZ tumors as compared to neu/WT tumors (Figure 6I,J). In addition, mRNA expression of direct E2F1 target genes, Rbl1 and Id1, was decreased in neu/HOZ tumors (Figure S4K).

Taken together, these results provide the first genetic evidence for the requirement of CIP2A for tumor formation and growth. Moreover, these results validates CIP2A's functional role as an *in vivo* inhibitor of senescence induction in breast cancer (Figure 6B-H).

CIP2A confers resistance of human breast tumors to senescence-inducing chemotherapy

Our results have thus far shown that CIP2A expression determines cellular senescence induction in response to p53 and p21 activation. To study the clinical relevance of these findings, the expression levels and the prognostic role for CIP2A was studied in a cohort of breast cancer tumor samples from the patients with advanced disease (n = 1010)(49). Interestingly, CIP2A was overexpressed in 79% of the breast cancers in this population of women (Figure 7A), of whom 89% had axillary node–positive breast cancer and the rest had high-risk node-negative cancer (49). This frequency is far greater than the frequency of CIP2A overexpression in unselected human breast cancers (approximately 40%; Figure 1B and 22). Also in this cohort, CIP2A expression significantly associates with high p53 immunopositivity (Figure 7A), and with several features linked with aggressive disease (Figure 7A). The difference in overall survival of patients with low or high CIP2A expression did not quite reach statistical significance in the entire patient population (p=0.073)(Figure S5A). However, in HER2-negative breast cancers, representing the great majority (77%) of the studied patient material (45), high tumor CIP2A expression significantly associated with poor overall survival (p=0.011)(Figure 7B) and distant recurrence or death (p=0.024)(Figure S5B). In multivariate analysis, assessing the independent role for CIP2A as a prognostic factor in Her2-negative breast cancers, tumor CIP2A expression tended to be associated with poor outcome (p=0.058; for CIP2A ++ vs. −, HR=4.26, 95% CI 1.29-14.08, p=0.017; for CIP2A ++ vs. +, HR=1.54, 95% CI 0.75-3.15, p=0.241), whereas tumor size (> 2.0 cm vs. ≤ 2.0 cm), axillary nodal status (positive vs. negative), histological grade (poorly vs. moderately vs. well differentiated) and p53 expression (positive vs. negative) were not associated with survival (p≥0.10 for each). However, absent ER expression was independently associated with poor survival in HER2-negative breast cancer (hazard ratio [HR] 2.18, 95% CI, 1.12-4.23, p=0.022). We speculate that CIP2A does not have prognostic value in HER2-positive cancers (p=0,687)(Figure S5C), even though it supports mammary tumorigenesis in HER2-driven mouse model (Figure 6E), because human cancers have more complex pattern of oncogenically active proteins; combined activity of which masks CIP2A's prognostic effect.

To study the role of tumor CIP2A in response of HER2-negative cancers to adjuvant therapy, association of CIP2A expression with survival of patients was studied in patient groups stratified by the type of chemotherapy administered (Figure 7C). In these groups, patients were randomly assigned to receive either single-agent docetaxel or vinorelbine (three cycles) followed (in both groups) by three cycles of fluorouracil, epirubicin, and

cyclophosphamide (FEC)(49). Notably, CIP2A overexpression significantly correlated with poor overall survival in the subgroup of patients who were assigned to receive vinorelbine followed by FEC (p=0,019)(Figure 7D), whereas CIP2A expression was not significantly associated with survival of patients assigned to docetaxel followed by FEC (p=0,373)(Figure S5D).

Vinorelbine is a semi-synthetic vinca alkaloid used to treat several kinds of human cancer types, including non-small cell lung cancer and advanced breast cancer (50, 51). Interestingly, another vinca alkaloid, vincristine, has been shown to induce senescence in MCF-7 cells (52). Based on this information, and the novel role for the E2F1-CIP2A feedback loop in preventing chemotherapy-induced senescence, we hypothesized that the favorable survival of the patients with CIP2A-negative cancer in the vinorelbine group could be linked with sensitivity of these cancers to vinorelbine-induced inhibition of E2F1. Indeed, vinorelbine treated MCF-7 cells mimicked the E2F1 and CIP2A inhibition-associated phenotype by displaying increased SA-beta-gal positivity and flattened cellular morphology (Figure 7E). Importantly, induction of senescence phenotype by vinorelbine was preceded by inhibition of both E2F1 and CIP2A protein expression at the 24h timepoint (Figure 7F). Interestingly, vinorelbine-induced E2F1 downregulation was not accompanied with either p53 or p21 induction (Figure 7G,S5E,F), but similarly to Nutlin-3 treatment, it was associated with inhibition of *e2f1* mRNA expression (Figure 7G). To study whether CIP2A deficient breast cancer cells are indeed more sensitive to vinorelbine-elicited E2F1 inhibition, MCF-7 cells transfected either with scrambled or CIP2A siRNA were treated with vinorelbine for 12 hours, at which timepoint vinorelbine did not yet inhibit CIP2A expression in parental cells (Figure 7H). As expected, CIP2A siRNA inhibited E2F1 protein expression in non-treated cells, and importantly CIP2A deficiency dramatically potentiated E2F1 downregulation in vinorelbine-treated cells (Figure 7H). Furthermore, exogenous CIP2A expression totally prevented E2F1 downregulation in vinorelbine-treated MCF-7 cells (Figure 7I).

These results demonstrate clinical relevance for CIP2A in progression and chemotherapy response of human breast cancers. Importantly, these results imply that CIP2A could be a useful predictive marker for selecting HER2-negative breast cancer patients, which currently lack efficient targeted therapy options, to vinca alkaloid-containing chemotherapy. Moreover, these results indicate that E2F1-CIP2A feedback mechanism is involved in chemotherapy resistance towards compounds that inhibit E2F1 expression independently of p53 or p21 activation.

Discussion

Mounting evidence indicates that the tumor suppression function of p53 relies on its capacity to induce senescence (1, 8-10, 53). In this study, we identify inhibition of CIP2A expression as a previously unrecognized mechanism required for senescence induction by activated p53 and p21 (Figure 7J). CIP2A's role as a functional p53 target is supported strongly by both unbiased bioinformatics analysis of the transcriptome in CIP2A depleted cells (Figure 1K), and by senescence experiments (Figure 3A,C,E,I and 5C,D). Importantly, CIP2A is positively regulated by p53 inactivation regardless of whether p53 activity is inhibited by Mdm2 (Figure 1D,E), mutations (Figure 1H), or by RNAi (Figure 1C). In addition to *in vitro* conditions, CIP2A expression correlates with p53 mutation in human breast cancer (Figure 1A,B and 7A), and *in vivo* re-activation of p53 in transgenic lymphomas expressing p53ER fusion protein potently inhibits CIP2A protein expression (Figure 1I and J). Furthermore, we demonstrate that loss of CIP2A restrics mammary carcinogenesis in a mouse model known to harbour p53 mutations (Figure 6E)(45). Moreover, a recent study demonstrated that in human gastric cancer CIP2A has the most

significant prognostic role in p53-immunopositive tumors (24). These findings together validate the *in vivo* relevance of CIP2A as a novel p53 target protein. Importantly, CIP2A is not a direct p53 target gene, but regulated via p21-E2F1 axis (Figure 2) albeit its expression is not sensitive to cell cycle inhibition (24). Moreover, we show that CIP2A inhibition is required for p21-induced senescence in p53 mutated cancer cells (Figures 4J,K). These results provide novel mechanistic explanation for recently demonstrated *in vivo* function for p21 in inducing senescence and delaying tumor onset (4, 54). Together, the results of this study strongly indicate that inhibition of CIP2A oncoprotein expression is a novel tumor suppression mechanism driven by the p53-p21 pathway (Figure 7J). Moreover, these results explain how inactivation of p53-p21 pathway promotes senescence resistance in cancer.

Inhibition of E2F transcriptional activity provokes senescence in human tumor cells and inhibits tumor growth (19-21). Nevertheless, E2F1 target genes involved in preventing senescence induction in cancer cells have been elusive. Our results show that activation of the p53-p21 pathway by Nutlin-3 induces simultaneously dephosphorylation of Rb, and transcriptional inhibition of *e2f1* gene expression (Figure 4A,B). We postulate that transcriptional inhibition of e2f1 by both Nutlin-3 and vinorelbine (Figure 4B and 7G) explains consequent inhibition of CIP2A expression, and triggers inhibition of a positive feedback loop between E2F1 and CIP2A (Figure 7J). Our data implicates that CIP2A supports E2F1 protein expression at the post-translational level both in human and mouse cells. Importantly, in addition to overexpression data, we also confirmed that CIP2A depletion caused inhibition of E2F1 protein expression (Figure 7H). In search of mechanistic explanation for CIP2A-mediated stabilization of E2F1 protein expression, we observed that CIP2A promotes E2F1 serine-364 phosphorylation, and this phosphorylation has been previously shown in another contexts to be associated with increased stability of E2F1 (17, 41). Moreover, we observed that inhibition of regulatory subunit of PP2A, B55α, increases E2F1 serine-364 phosphorylation and reverses Nutlin-3 induced downregulation of E2F1 (Figure 4F,G). Previously, we showed that inhibition of B55α reverses CIP2A depletion induced anti-proliferative and gene expression effects (34). Interestingly, deletion of B55α gene was recently identified as a potential driver mutation specifically in luminal B type of breast cancer (55). These results indicate that B55α containing PP2A tumor suppressor complex needs to be inhibited during breast cancer progression either by genetic mutations or via overexpression of CIP2A. Importantly, our data indicate that also other mechanisms, than p53 inactivation-induced E2F1 expression, may drive high CIP2A expression in human breast cancer (Fig. 1B and 7A). We postulate that in these cases ETS-1 and MYC-mediated CIP2A expression (24, 30) supports E2F1 expression and thereby confers these cells resistant to senescence induction (see Figure 7J for schematic presentation).

Although CIP2A expression has been shown to predict for poor patient survival in many different human cancer types (24, 28)(Table S1), such evidence has thus far been lacking for breast cancer. In this study we demonstrate that CIP2A has a prognostic role in HER2-negative breast cancer in which there is high demand for novel therapy targets. Interestingly, low E2F1 mRNA expression levels were found specifically in HER2-negative breast tumors (56). Therefore, it can be envisioned that the prognostic value of CIP2A becomes more apparent in HER2-negative cancers in which CIP2A-mediated post-translational increase of E2F1 protein becomes critical for tumor progression. Moreover, the observation that E2F1 response to senescence-inducing vinorelbine chemotherapy is dependent on the CIP2A status provides a plausible mechanistic explanation for the favourable survival of patients having CIP2A/HER2-negative breast cancer, and who were treated with vinorelbine prior FEC (Figure 7D).

Pro-senescence therapies are emerging as an alternative approach for cancer treatment (6, 7). However, the majority of the thus far suggested strategies for therapeutic senescence

induction rely on activation of p53 and other cellular checkpoint mechanisms (6, 7). Although hypothetically reasonable, these strategies suffer from serious shortcoming due to fact that in the majority of human cancers several checkpoint mechanisms are functionally impaired. Therefore, identification of the E2F1-CIP2A positive feedback loop as a novel pro-senescence therapy target mechanism that functions downstream of inactivated p53, and which inhibition induces senescence independently of p53 activation, is a fundamentally important finding. As an example of *in vivo* importance of the p53-independent senescence inducing mechanisms, Pandolfi and co-workers recently demonstrated a role for p21-induced senescence in tumor suppression (4). In that regard, our data show that CIP2A expression not only inhibits p53-induced senescence (Figure 3E,F and I,J), but also p21-induced senescence in p53-mutant breast cancer cells (Figure 4J,K). Since p53 inhibition promotes CIP2A expression (Figures 1 and 2), these results together indicate that senescence resistance in p53 mutant tumors is caused by a combined effect of impaired p53 checkpoint activity, and increased activity of the E2F1-CIP2A feedback loop. Thereby CIP2A deregulation could be considered as a novel gain-of-function for mutant p53 in cancer (13). Importantly, the feasibility of targeting the identified E2F1-CIP2A positive feedback loop for pro-senescence therapy is supported by the lack of any obvious developmental defects in the CIP2A knock-down mouse used in this study (Figure S4)(44). Moreover, as CIP2A is overexpressed at an exceptionally high frequency in 65-90 % of tumor samples of most major human cancer types (Table S1), its inhibition could serve as a general strategy to sensitize cancer cells to pro-senescence therapies. These conclusions are supported by previously reported increase in SA-beta-gal activity in CIP2A-depleted gastric cancer cell line (57).

Taken together, this study identifies a hitherto unrecognized oncogenic mechanism downstream of inactivated p53-p21 pathway. Our results demonstrate that whereas in E2F1 stimulates CIP2A expression in cells with inactive p53-p21 pathway, inhibition of the E2F1-CIP2A feedback loop is essential for senescence induction (Figure 7J). Moreover, as inhibition of the E2F1-CIP2A feedback loop induces senescence also in p53 mutant cells, and pRb is not needed for CIP2A inhibition-induced senescence (Figure S3), these results indicate that inhibition of E2F1 and CIP2A can induce senescence in cancer cells without activation of upstream p53-p21-pRb pathway. In general, these results indicate that senescence induction in cancer cells is determined, rather than simply by strength of the senescence inducing stimuli, by the activity of this newly identified feedback mechanism between E2F1 and CIP2A (Figure 7J). Finally, results of this study should encourage development of approaches both to target E2F1-CIP2A feedback mechanism, and to stratify patients to senescence-inducing cancer therapies based on tumor CIP2A status.

Methods

Cell culture and drug treatments

MCF-7, MDA-MB-231, HeLa and SAOS-2 cell lines were obtained from ATCC. HCT116 and its clonal p53 (p53-/-) and p21 (p21-/-) deletion mutants were kindly provided by Prof. B. Vogelstein. Cells were tested twice a year as negative for mycoplasmas and acholeplasmas with Mycoplasma Detection Kit (Roche). Cells were exposed to indicated concentration of Nutlin-3 (Cayman Chemicals), doxorubicin (Sigma), vinorelbine (Sigma) or RITA (Cayman Chemicals).

Antibodies

For immunoblotting following antibodies were used: CIP2A: rabbit polyclonal (Soo Hoo, et al. 2002) and mouse monoclonal 2G10-3B5 (Santa Cruz), p21: rabbit polyclonal C-19 (Santa Cruz), p53: mouse monoclonal DO-1 (Santa Cruz) and rabbit polyclonal CM5

(Vector Laboratories), β-actin: mouse monoclonal (Sigma), Rb: rabbit polyclonal C-15 (Santa Cruz), B55α: mouse monoclonal 2G9 (Cell Signaling), Ser 807/811 phosphorylated Rb: rabbit polyclonal (Santa Cruz), E2F1 KH95: mouse monoclonal (Santa Cruz), Ser 364 phosphorylated E2F1: rabbit polyclonal (Abcam), DcR2: rabbit polyclonal (Abcam).

Immunohistochemical and statistical analysis of human breast cancer patient samples

CIP2A immunostaining in both FinProg and in FinHer breast cancer patient cohorts were performed by polyclonal rabbit antibody (58). CIP2A were immunostained and analyzed from both cohort of human breast cancer patient tumor samples (FinProg and FinHer studies) as described previously (34). In the FinProg cohort of breast cancer patients p53 and KI67 immunostainings from breast tumors and analysis of tumor size and tumor gradus were performed as previously described (59). In the FinHer cohort of breast cancer patients HER2 and KI67 immunostainings, analysis of tumor diameter, tumor size and tumor gradus as well as statistical analysis of total and cumulative survival and percentage of alive patients in different subgroups were performed similarly as previously (49). P53 immunostainings from FinHer cohort was done following same protocol as have been published for FinProg study (59). An ethics committee at Helsinki University hospital approved the FinHer study (HUCH 426/E6/00). Regarding FinProg material permission to use formalin fixed paraffin-embedded tissues for research purposes was provided by the Ministry of Social Affairs and Health, Finland (permission 123/08/97).

Animal experiments

MMTVneu mice (60) expressing oncogenic HER2 under the control of the mouse mammary tumor virus promoter specifically in the mouse mammary gland were purchased from The Jackson Laboratory and crossed with CIP2A heterozygous genetrap hypomorphic mutant mice ($CIP2A^{HEZ}$)(44). MMTVneu/$CIP2A^{HEZ}$ mice were intercrossed to produce MMTVneu/$CIP2A^{WT}$, MMTVneu/$CIP2A^{HEZ}$ and MMTVneu/$CIP2A^{HOZ}$ mice. Mice were genotyped by PCR analysis of genomic DNA for MMTVneu transgene according to The Jackson Laboratory's protocol and for CIP2A genetrap as previously described(44). CIP2A genotyping results were confirmed with mRNA analysis by RT-PCR. Mice were checked for tumor appearance twice a week. Formed tumors were palpated twice a week and mice were sacrified when tumor diameter reached 20mm. Tumor size was measured by palpating and by weighting after sacrificing and preparation from mouse. Immunohistochemical staining for Ki67, DcR2 and hematoxylin and eosin (H&E) staining were performed as previously described (41). Tumor cells were isolated by forcing cells through a 70μm-pore filter (BD Biosciences). Cells were cultured with DMEM/F12 Ham containing 10% of serum, insulin, hydrocortisone and mouse epidermal growth factor. Mouse embryonal fibroblasts were isolated from WT and CIP2A HOZ embryos at 13,5 days of gestation, and cultured in DMEM containing 15% of serum.

In DMBA treatment dorsal skin of WT and $CIP2A^{HOZ}$ mice were treated with DMBA (20μg in 200μof acetone) three times a week for two weeks. A day before the first treatment mouse back was shawed and mice were sacrified 24 hours after the last treatment. Lymphoma lysates from either tamoxifen or peanut oil systemically treated EuMyc:p53ER mice were prepared as described previously (33). All animal work protocols were approved by the Regional State Administrative Agency for Southern Finland (ESLH-2007-08517, ESLH-2009-00515/Ym-23).

Proliferation assay and SA-beta-gal staining

Proliferation capacity of MEFs was studied by calculating cell numbers of MEFs from 3 different wild type (WT) and $CIP2A^{HOZ}$ embryos seeded to 14000 cell/cm^2 and divided when 70-80% confluent. Cells were cultured for 46 days. In order to detect senescent cells,

cells and mouse skin sections were fixed and stained for senescence associated-beta-galactoside (SA-beta-gal) at pH 6.0 (Sigma) according to manufacturer's protocol. Senescent cells in in vitro assays were quantified under the microscope by counting morphologically flattened and SA-beta-gal positive cells. SA-beta-gal staining in mouse skin were quantitated by counting positively stained areas from two to three sections per mouse.

Supplementary Material

Refer to Web version on PubMed Central for supplementary material.

Acknowledgments

We thank Taina Kalevo-Mattila and Inga Pukonen for expert technical assistance. Turku Disease Model Center (TCDM) is acknowledged for expert assistance in mouse work. Dr. Ventelä is thanked for help in mouse analysis. We thank Dr. Vogelstein for HCT116 clones. Drs. Stein Aerts, Annelien Verfaillie and Eran Andrecheck are greatly acknowledged for sharing their unpublished data. This study was supported by grants from the Academy of Finland (grant no. 8217676, 122546 and 137687), Sigrid Juselius Foundation, the Cancer Society of Finland, Association of International Cancer Research (grant no. 08-0614), Helsinki University Central Hospital Research Funds (TYH2009304), Turku University Hospital (project 13336), and Foundation of the Finnish Cancer Institute.

References

1. Larsson LG. Oncogene- and tumor suppressor gene-mediated suppression of cellular senescence. Semin Cancer Biol. 2011; 21:367–76. [PubMed: 22037160]
2. Michaloglou C, Vredeveld LC, Soengas MS, Denoyelle C, Kuilman T, van der Horst CM, et al. BRAFE600-associated senescence-like cell cycle arrest of human naevi. Nature. 2005; 436:720–4. [PubMed: 16079850]
3. Sun P, Yoshizuka N, New L, Moser BA, Li Y, Liao R, et al. PRAK is essential for ras-induced senescence and tumor suppression. Cell. 2007; 128:295–308. [PubMed: 17254968]
4. Lin HK, Chen Z, Wang G, Nardella C, Lee SW, Chan CH, et al. Skp2 targeting suppresses tumorigenesis by Arf-p53-independent cellular senescence. Nature. 2010; 464:374–9. [PubMed: 20237562]
5. Alimonti A, Nardella C, Chen Z, Clohessy JG, Carracedo A, Trotman LC, et al. A novel type of cellular senescence that can be enhanced in mouse models and human tumor xenografts to suppress prostate tumorigenesis. J Clin Invest. 2010; 120:681–93. [PubMed: 20197621]
6. Ewald JA, Desotelle JA, Wilding G, Jarrard DF. Therapy-induced senescence in cancer. J Natl Cancer Inst. 2010; 102:1536–46. [PubMed: 20858887]
7. Nardella C, Clohessy JG, Alimonti A, Pandolfi PP. Pro-senescence therapy for cancer treatment. Nat Rev Cancer. 2011; 11:503–11. [PubMed: 21701512]
8. Brady CA, Jiang D, Mello SS, Johnson TM, Jarvis LA, Kozak MM, et al. Distinct p53 transcriptional programs dictate acute DNA-damage responses and tumor suppression. Cell. 2011; 145:571–83. [PubMed: 21565614]
9. Post SM, Quintas-Cardama A, Terzian T, Smith C, Eischen CM, Lozano G. p53-dependent senescence delays Emu-myc-induced B-cell lymphomagenesis. Oncogene. 2010; 29:1260–9. [PubMed: 19935700]
10. Xue W, Zender L, Miething C, Dickins RA, Hernando E, Krizhanovsky V, et al. Senescence and tumour clearance is triggered by p53 restoration in murine liver carcinomas. Nature. 2007; 445:656–60. [PubMed: 17251933]
11. Ventura A, Kirsch DG, McLaughlin ME, Tuveson DA, Grimm J, Lintault L, et al. Restoration of p53 function leads to tumour regression in vivo. Nature. 2007; 445:661–5. [PubMed: 17251932]
12. Robles AI, Harris CC. Clinical outcomes and correlates of TP53 mutations and cancer. Cold Spring Harbor perspectives in biology. 2010; 2:a001016. [PubMed: 20300207]
13. Oren M, Rotter V. Mutant p53 gain-of-function in cancer. Cold Spring Harbor perspectives in biology. 2010; 2:a001107. [PubMed: 20182618]

14. Lane DP, Cheok CF, Lain S. p53-based cancer therapy. Cold Spring Harbor perspectives in biology. 2010; 2:a001222. [PubMed: 20463003]
15. Polager S, Ginsberg D. p53 and E2f: partners in life and death. Nat Rev Cancer. 2009; 9:738–48. [PubMed: 19776743]
16. Mundle SD, Saberwal G. Evolving intricacies and implications of E2F1 regulation. Faseb J. 2003; 17:569–74. [PubMed: 12665469]
17. Stevens C, Smith L, La Thangue NB. Chk2 activates E2F-1 in response to DNA damage. Nat Cell Biol. 2003; 5:401–9. [PubMed: 12717439]
18. Huang B, Deo D, Xia M, Vassilev LT. Pharmacologic p53 activation blocks cell cycle progression but fails to induce senescence in epithelial cancer cells. Mol Cancer Res. 2009; 7:1497–509. [PubMed: 19737973]
19. Maehara K, Yamakoshi K, Ohtani N, Kubo Y, Takahashi A, Arase S, et al. Reduction of total E2F/DP activity induces senescence-like cell cycle arrest in cancer cells lacking functional pRB and p53. J Cell Biol. 2005; 168:553–60. [PubMed: 15716376]
20. Park C, Lee I, Kang WK. E2F-1 is a critical modulator of cellular senescence in human cancer. International journal of molecular medicine. 2006; 17:715–20. [PubMed: 16596252]
21. Vernier M, Bourdeau V, Gaumont-Leclerc MF, Moiseeva O, Begin V, Saad F, et al. Regulation of E2Fs and senescence by PML nuclear bodies. Genes Dev. 2011; 25:41–50. [PubMed: 21205865]
22. Come C, Laine A, Chanrion M, Edgren H, Mattila E, Liu X, et al. CIP2A is associated with human breast cancer aggressivity. Clin Cancer Res. 2009; 15:5092–100. [PubMed: 19671842]
23. Junttila MR, Puustinen P, Niemela M, Ahola R, Arnold H, Bottzauw T, et al. CIP2A inhibits PP2A in human malignancies. Cell. 2007; 130:51–62. [PubMed: 17632056]
24. Khanna A, Bockelman C, Hemmes A, Junttila MR, Wiksten JP, Lundin M, et al. MYC-dependent regulation and prognostic role of CIP2A in gastric cancer. J Natl Cancer Inst. 2009; 101:793–805. [PubMed: 19470954]
25. Ma L, Wen ZS, Liu Z, Hu Z, Ma J, Chen XQ, et al. Overexpression and small molecule-triggered downregulation of CIP2A in lung cancer. PLoS ONE. 2011; 6:e20159. [PubMed: 21655278]
26. Mathiasen DP, Egebjerg C, Andersen SH, Rafn B, Puustinen P, Khanna A, et al. Identification of a c-Jun N-terminal kinase-2-dependent signal amplification cascade that regulates c-Myc levels in ras transformation. Oncogene. 2012; 31:390–401. [PubMed: 21706057]
27. Junttila MR, Westermarck J. Mechanisms of MYC stabilization in human malignancies. Cell Cycle. 2008; 7:592–6. [PubMed: 18256542]
28. Lucas CM, Harris RJ, Giannoudis A, Copland M, Slupsky JR, Clark RE. Cancerous inhibitor of PP2A (CIP2A) at diagnosis of chronic myeloid leukemia is a critical determinant of disease progression. Blood. 2011; 117:6660–8. [PubMed: 21490338]
29. Sihto H, Kukko H, Koljonen V, Sankila R, Bohling T, Joensuu H. Merkel cell polyomavirus infection, large T antigen, retinoblastoma protein and outcome in Merkel cell carcinoma. Clin Cancer Res. 2011; 17:4806–13. [PubMed: 21642382]
30. Khanna A, Okkeri J, Bilgen T, Tiirikka T, Vihinen M, Visakorpi T, et al. ETS1 mediates MEK1/2-dependent overexpression of cancerous inhibitor of protein phosphatase 2A (CIP2A) in human cancer cells. PLoS ONE. 2011; 6:e17979. [PubMed: 21445343]
31. Vassilev LT, Vu BT, Graves B, Carvajal D, Podlaski F, Filipovic Z, et al. In vivo activation of the p53 pathway by small-molecule antagonists of MDM2. Science. 2004; 303:844–8. [PubMed: 14704432]
32. Issaeva N, Bozko P, Enge M, Protopopova M, Verhoef LG, Masucci M, et al. Small molecule RITA binds to p53, blocks p53-HDM-2 interaction and activates p53 function in tumors. Nat Med. 2004; 10:1321–8. [PubMed: 15558054]
33. Martins CP, Brown-Swigart L, Evan GI. Modeling the therapeutic efficacy of p53 restoration in tumors. Cell. 2006; 127:1323–34. [PubMed: 17182091]
34. Niemela M, Kauko O, Sihto H, Mpindi JP, Nicorici D, Pernila P, et al. CIP2A signature reveals the MYC dependency of CIP2A-regulated phenotypes and its clinical association with breast cancer subtypes. Oncogene. 2012; 31:4266–78. [PubMed: 22249265]

35. Johnson AC, Murphy BA, Matelis CM, Rubinstein Y, Piebenga EC, Akers LM, et al. Activator protein-1 mediates induced but not basal epidermal growth factor receptor gene expression. Mol Med. 2000; 6:17–27. [PubMed: 10803405]
36. Helmbold H, Komm N, Deppert W, Bohn W. Rb2/p130 is the dominating pocket protein in the p53-p21 DNA damage response pathway leading to senescence. Oncogene. 2009; 28:3456–67. [PubMed: 19648966]
37. Kim KS, Seu YB, Baek SH, Kim MJ, Kim KJ, Kim JH, et al. Induction of cellular senescence by insulin-like growth factor binding protein-5 through a p53-dependent mechanism. Mol Biol Cell. 2007; 18:4543–52. [PubMed: 17804819]
38. Li Q, Tang L, Roberts PC, Kraniak JM, Fridman AL, Kulaeva OI, et al. Interferon regulatory factors IRF5 and IRF7 inhibit growth and induce senescence in immortal Li-Fraumeni fibroblasts. Mol Cancer Res. 2008; 6:770–84. [PubMed: 18505922]
39. Choi YA, Park JS, Park MY, Oh KS, Lee MS, Lim JS, et al. Increase in CIP2A expression is associated with doxorubicin resistance. FEBS Lett. 2011
40. Johnson DG, Ohtani K, Nevins JR. Autoregulatory control of E2F1 expression in response to positive and negative regulators of cell cycle progression. Genes Dev. 1994; 8:1514–25. [PubMed: 7958836]
41. Kontaki H, Talianidis I. Lysine methylation regulates E2F1-induced cell death. Mol Cell. 2010; 39:152–60. [PubMed: 20603083]
42. Westermarck J, Hahn WC. Multiple pathways regulated by the tumor suppressor PP2A in transformation. Trends in molecular medicine. 2008; 14:152–60. [PubMed: 18329957]
43. Lodygin D, Menssen A, Hermeking H. Induction of the Cdk inhibitor p21 by LY83583 inhibits tumor cell proliferation in a p53-independent manner. J Clin Invest. 2002; 110:1717–27. [PubMed: 12464677]
44. Ventela S, Come C, Makela JA, Hobbs RM, Mannermaa L, Kallajoki M, et al. CIP2A Promotes Proliferation of Spermatogonial Progenitor Cells and Spermatogenesis in Mice. PLoS ONE. 2012; 7:e33209. [PubMed: 22461891]
45. Li B, Rosen JM, McMenamin-Balano J, Muller WJ, Perkins AS. neu/ERBB2 cooperates with p53-172H during mammary tumorigenesis in transgenic mice. Mol Cell Biol. 1997; 17:3155–63. [PubMed: 9154814]
46. Ansieau S, Bastid J, Doreau A, Morel AP, Bouchet BP, Thomas C, et al. Induction of EMT by twist proteins as a collateral effect of tumor-promoting inactivation of premature senescence. Cancer Cell. 2008; 14:79–89. [PubMed: 18598946]
47. Kuilman T, Michaloglou C, Mooi WJ, Peeper DS. The essence of senescence. Genes Dev. 2010; 24:2463–79. [PubMed: 21078816]
48. Swarbrick A, Roy E, Allen T, Bishop JM. Id1 cooperates with oncogenic Ras to induce metastatic mammary carcinoma by subversion of the cellular senescence response. Proc Natl Acad Sci U S A. 2008; 105:5402–7. [PubMed: 18378907]
49. Joensuu H, Kellokumpu-Lehtinen PL, Bono P, Alanko T, Kataja V, Asola R, et al. Adjuvant docetaxel or vinorelbine with or without trastuzumab for breast cancer. The New England journal of medicine. 2006; 354:809–20. [PubMed: 16495393]
50. Galano G, Caputo M, Tecce MF, Capasso A. Efficacy and tolerability of vinorelbine in the cancer therapy. Current drug safety. 2011; 6:185–93. [PubMed: 22122393]
51. Kellokumpu-Lehtinen PL, Sunela K, Lehtinen I, Joensuu H, Sjostrom-Mattson J. A phase I study of an all-oral combination of vinorelbine/capecitabine in patients with metastatic breast cancer previously treated with anthracyclines and/or taxanes. Clinical breast cancer. 2006; 7:401–5. [PubMed: 17239265]
52. Groth-Pedersen L, Ostenfeld MS, Hoyer-Hansen M, Nylandsted J, Jaattela M. Vincristine induces dramatic lysosomal changes and sensitizes cancer cells to lysosome-destabilizing siramesine. Cancer Res. 2007; 67:2217–25. [PubMed: 17332352]
53. Chen Z, Trotman LC, Shaffer D, Lin HK, Dotan ZA, Niki M, et al. Crucial role of p53-dependent cellular senescence in suppression of Pten-deficient tumorigenesis. Nature. 2005; 436:725–30. [PubMed: 16079851]

54. Barboza JA, Liu G, Ju Z, El-Naggar AK, Lozano G. p21 delays tumor onset by preservation of chromosomal stability. Proc Natl Acad Sci U S A. 2006; 103:19842–7. [PubMed: 17170138]

55. Curtis C, Shah SP, Chin SF, Turashvili G, Rueda OM, Dunning MJ, et al. The genomic and transcriptomic architecture of 2,000 breast tumours reveals novel subgroups. Nature. 2012; 486:346–52. [PubMed: 22522925]

56. Vuaroqueaux V, Urban P, Labuhn M, Delorenzi M, Wirapati P, Benz CC, et al. Low E2F1 transcript levels are a strong determinant of favorable breast cancer outcome. Breast Cancer Res. 2007; 9:R33. [PubMed: 17535433]

57. Li W, Ge Z, Liu C, Liu Z, Bjorkholm M, Jia J, et al. CIP2A is overexpressed in gastric cancer and its depletion leads to impaired clonogenicity, senescence, or differentiation of tumor cells. Clin Cancer Res. 2008; 14:3722–8. [PubMed: 18559589]

58. Soo Hoo L, Zhang JY, Chan EK. Cloning and characterization of a novel 90 kDa 'companion' auto-antigen of p62 overexpressed in cancer. Oncogene. 2002; 21:5006–15. [PubMed: 12118381]

59. Sihto H, Lundin J, Lehtimaki T, Sarlomo-Rikala M, Butzow R, Holli K, et al. Molecular subtypes of breast cancers detected in mammography screening and outside of screening. Clin Cancer Res. 2008; 14:4103–10. [PubMed: 18593987]

60. Guy CT, Webster MA, Schaller M, Parsons TJ, Cardiff RD, Muller WJ. Expression of the neu protooncogene in the mammary epithelium of transgenic mice induces metastatic disease. Proc Natl Acad Sci U S A. 1992; 89:10578–82. [PubMed: 1359541]

Europe PMC Funders Author Manuscripts

Europe PMC Funders Author Manuscripts

Statement of significance

It has been recently realized that most of the currently used chemotherapies exert their therapeutic effect at least partly by induction of terminal cell arrest, senescence. However, the mechanisms by which cell intrinsic senescence sensitivity is determined are poorly understood. Results of this study identify E2F1-CIP2A positive feedback loop, as a key determinant of breast cancer cell sensitivity to senescence and growth arrest induction. Our data also indicates that this newly characterized interplay between two frequently overexpressed oncoproteins, constitutes a promising pro-senescence target for therapy of cancers with inactivated p53 and p21. Finally, these results may also facilitate novel patient stratification strategies for selection of patients to senescence-inducing cancer therapies.

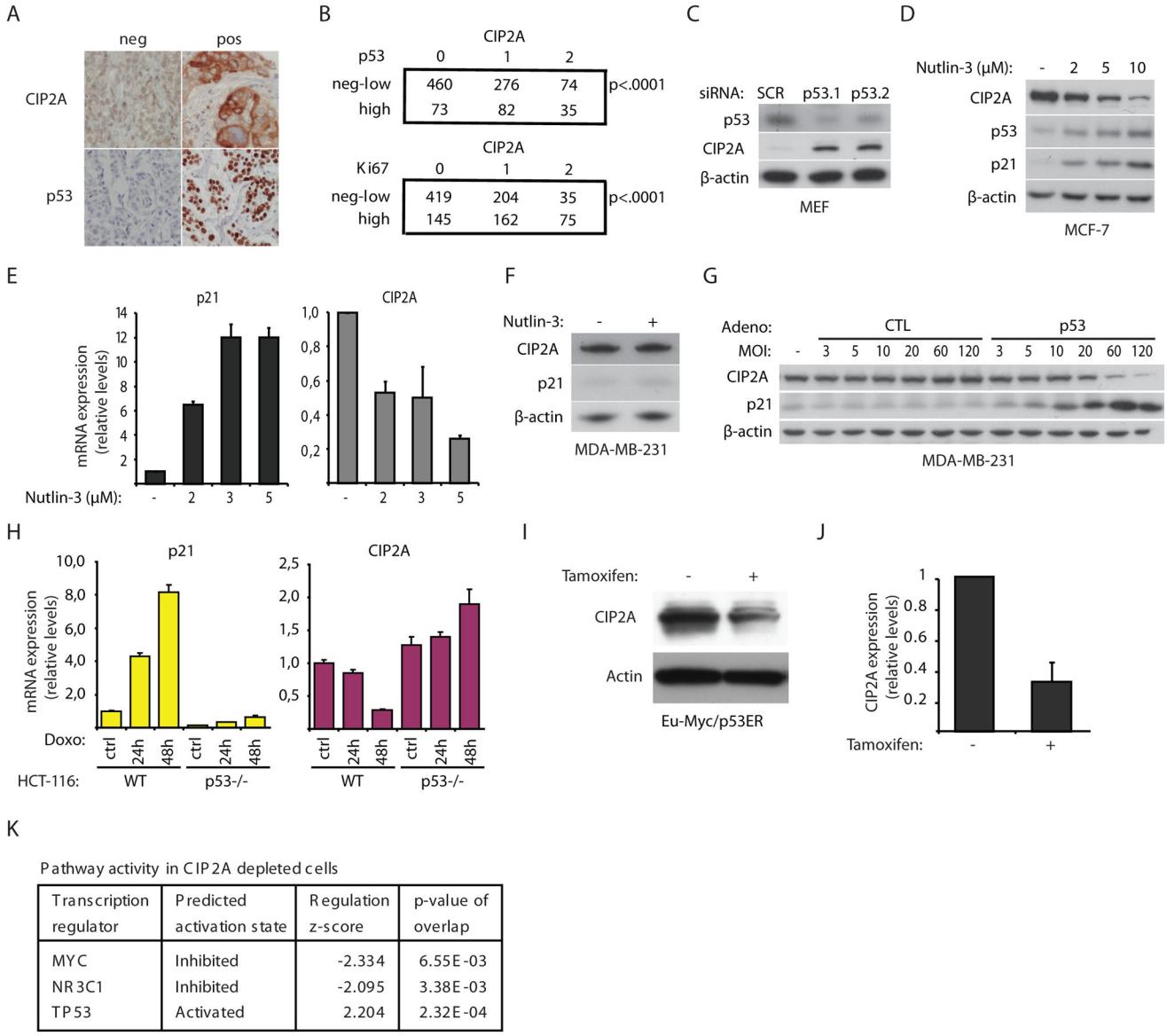

Figure 1. Wild type p53 negatively regulates CIP2A expression

A) Representative immunohistochemical stainings of CIP2A and p53 expression in human breast cancer tumors. **B)** CIP2A expression positively correlates with p53 expression and with proliferation marker Ki67 in human breast tumors (n=1228). P value calculated by chi-squared test. **C)** Western blot analysis of CIP2A expression in mouse embryonal fibroblasts (MEFs) 48h after transfection with scrambled (SCR) or two different p53 siRNAs (p53.1 and p53.2). **D)** Western blot analysis of CIP2A, p53 and p21 expression in MCF-7 cells treated with 2, 5 or 10μM of Nutlin-3 for 36h. **E)** p21 and CIP2A mRNA expression in MCF-7 cells treated with 2, 3, and 5μM of Nutlin-3 for 24h. Shown is mean +SEM of two independent experiments. **F)** CIP2A protein expression in MDA-MB-231 human breast cancer cells harboring DNA-binding deficient p53 treated with 5 μM of Nutlin-3 for 24 hours. **G)** Western blot analysis of CIP2A expression in MDA-MB-231 cells 48h after transduction either with control (CTL) or wild-type p53 expressing (p53) adeno virus using different MOIs. **H)** p21 and CIP2A mRNA expression from wild-type (WT) and p53-/-

Europe PMC Funders Author Manuscripts

HCT-116 cells treated with 0,2μg/μl of doxorubicin for 0 (ctrl), 24 or 48h. Shown is mean +SD of two experiments analyzed by qBasePLUS 1.0 analysis software. **I)** Representative western blot analysis of CIP2A expression from tamoxifen-inducible Eu-Myc:p53ER lymphomas treated systemically either with vehicle (−) or with tamoxifen (+). **J)** Quantitation of CIP2A protein levels from figure **(I)**. CIP2A protein expression normalized to β-actin. Shown is mean +SD of three vehicle and four tamoxifen treated lymphoma lysates. **K)** Ingenuity transcription factor analysis of CIP2A regulated gene expression changes in HeLa cells. **C,D,G)** Shown is a representative result of two independent experiments with similar results.

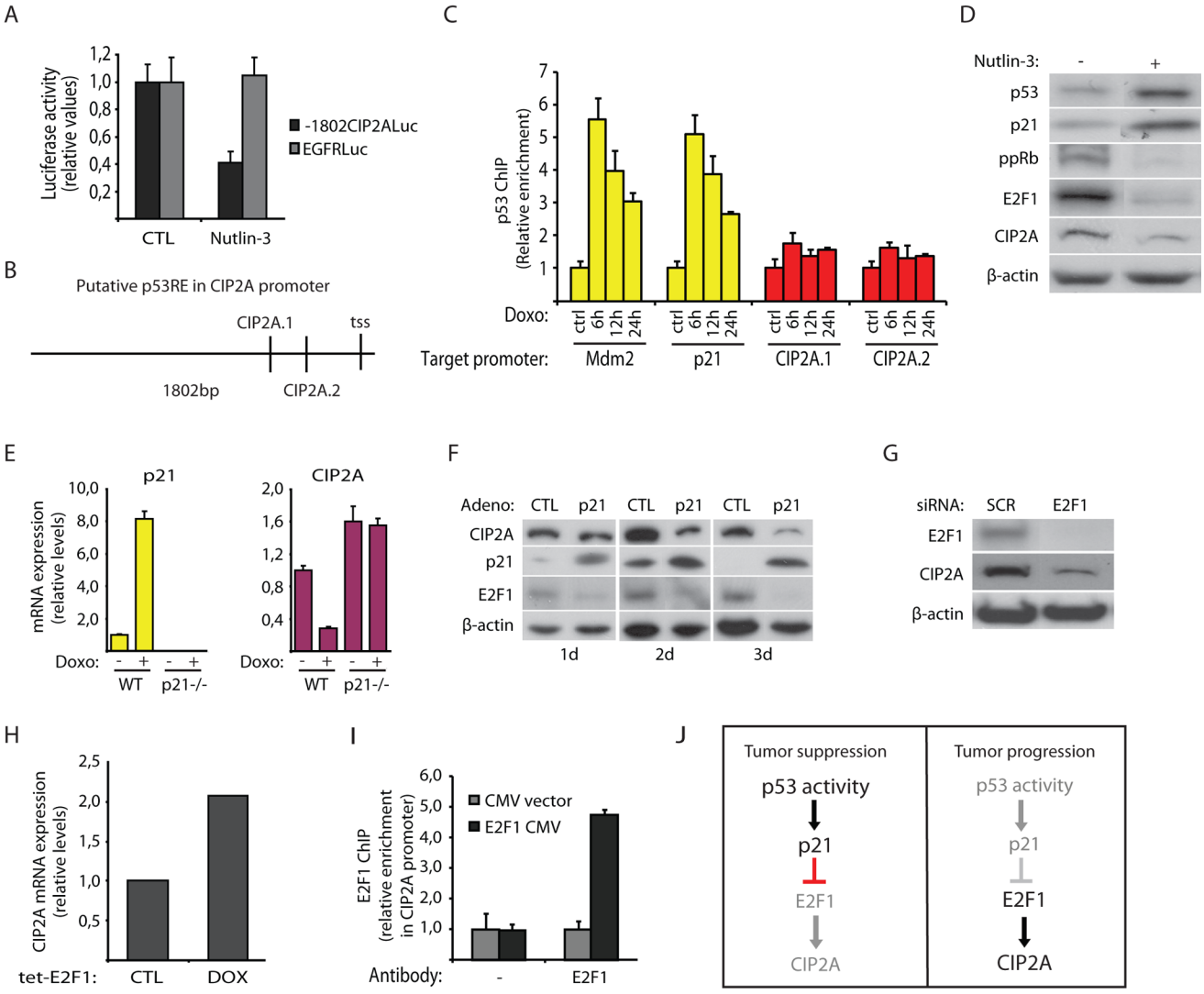

Figure 2. E2F1 upregulates CIP2A expression downstream of inactivated p53

A) MCF-7 cells transfected either with CIP2A promoter (-1802CIP2Aluc) or epidermal growth factor receptor promoter (EGFRluc) luciferase reporter plasmid were treated with Nutlin-3 (2μM) for 24h and luciferase activity was measured. Shown is mean +SD of two independent experiments. **B)** Putative p53 responsive elements in CIP2A −1802 promoter according to Genomatix and ConTra softwares (tss= transcription start site). **C)** ChIP was performed with p53 antibody from HCT-116 cells treated with 0,2 μg/ml of doxorubicin for 0 (ctrl), 6, 12 or 24 hours. ChIP DNA was analyzed by real-time PCR with two different set of primers against putative p53 binding sites in CIP2A promoter and as a positive control against p53 binding site in p21 and Mdm2 promoters. Results were analyzed by qBasePLUS 1.0 analysis software and shown is mean +SD from a representative of two independent experiments. **D)** Western blot detecting p53, p21, phosphorylated (Ser807/Ser811) Rb (ppRb), E2F1 and CIP2A expression from MCF-7 cells treated with 3μM of Nutlin-3 for 8 hours. Irrelevant data has been removed from the original graph. **E)** p21 and CIP2A mRNA expression analyzed by RT PCR from isogenic wild-type (WT) and p21-/- HCT-116 cells treated with 0,2μg/ml of doxorubicin for 48 h. Shown is mean +SD of two experiments analyzed by qBasePLUS 1.0 analysis software. **F)** Western blot analysis of CIP2A, p21,

E2F1 and β-actin expression from MDA-MB-231 cells transduced either with control (CTL) or p21 expressing adeno vectors (p21) with MOI 80 for 1, 2 or 3 days. Irrelevant data has been removed from the original graph. **G)** Western blot analysis of CIP2A and E2F1 expression in MCF-7 cells 24 hours after transfection either with scrambled (SCR) or E2F1 siRNA. Irrelevant data has been removed from the original graph. **H)** CIP2A mRNA expression in doxicycline-inducible wild-type E2F1 expressing Saos-2 cells treated for 24 hours with doxicycline (DOX). **I)** E2F1 ChIP was performed in Saos-2 cells transfected either with empty CMV vector or with CMV vector expressing E2F1 (E2F1 CMV). Shown is mean +SD of replicates from a representative of two experiments with similar results. **J)** Schematic model of CIP2A regulation by p53 activity. Inactive molecules and functions are shown in grey. **D,F,G)** Shown is a representative result of two independent experiments with similar results.

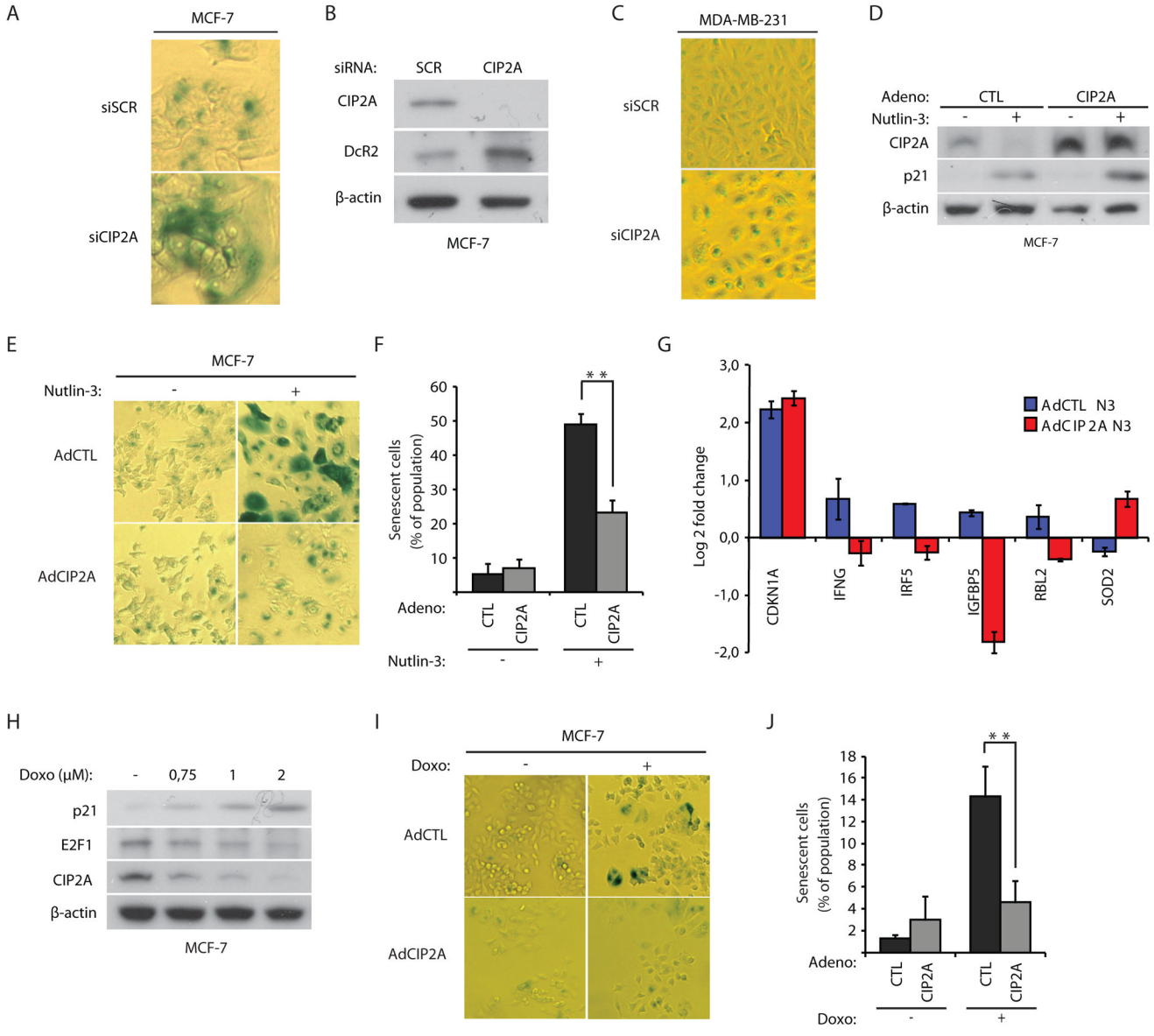

Figure 3. Inhibition of CIP2A expression is a prerequisite for p53-mediated senescence induction

A) SA-beta-gal staining of MCF-7 cells 5 days after transfection either with scrambled (siSCR) or CIP2A siRNA (siCIP2A). **B)** Western blot analysis of senescence marker DcR2 expression in MCF-7 cells 5 days after transfection either with scrambled (SCR) or with CIP2A (CIP2A) siRNA. **C)** SA-beta-gal staining of MDA-MB-231 cells 5 days after transfection either with scrambled (siSCR) or CIP2A siRNA (siCIP2A). **D)** Western blot analysis of CIP2A and p21 expression in either control (AdCTL) or CIP2A (AdCIP2A) transduced (MOI=40) MCF-7 cells treated with Nutlin-3 (3μM) for 3 days. Irrelevant data has been removed from the original graph. **E)** SA-beta-gal staining of AdCTL or AdCIP2A transduced (MOI=40) MCF-7 cells treated with Nutlin-3 (3μM) for 3 days. **F)** Percentage of SA-β-gal positive and morphologically flattened cells of AdCTL or AdCIP2A transduced (MOI=40) MCF-7 cells treated with Nutlin-3 (3μM) for 3 days. Shown is mean +SD from two experiment. ** p=0,0022 by Student's t-test. **G)** RT-PCR analysis of cellular senescence associated p53-regulated genes IFNG, IRF5, IGFBP5, RBL2 and SOD2 from AdCTL or

Europe PMC Funders Author Manuscripts

AdCIP2A transduced (MOI=40) MCF-7 cells treated with Nutlin-3 for 3 days. Shown is log2 fold change +SEM of two replicates from a representative experiment of **(E). H)** Western blot analysis of CIP2A, p21 and E2F1 expression in MCF-7 cells treated with Doxorubicin (Doxo) with indicated concentrations. **I)** SA-beta-gal staining of AdCTL or AdCIP2A transduced (MOI=40) MCF-7 cells treated with doxorubicin (2uM) for 3 days. **J)** Percentage of SA-β-gal positive and morphologically flattened cells of AdCTL or AdCIP2A transduced (MOI=40) MCF-7 cells treated with doxorubicin (2μM) for 3 days. Shown is mean +SD of three replicates from a representative experiment in **(I)** . ** p=0,0082 by Student's t-test. **A,B,C,D,E,H,I)** Shown is a representative result of at least two independent experiments with similar results.

Europe PMC Funders Author Manuscripts

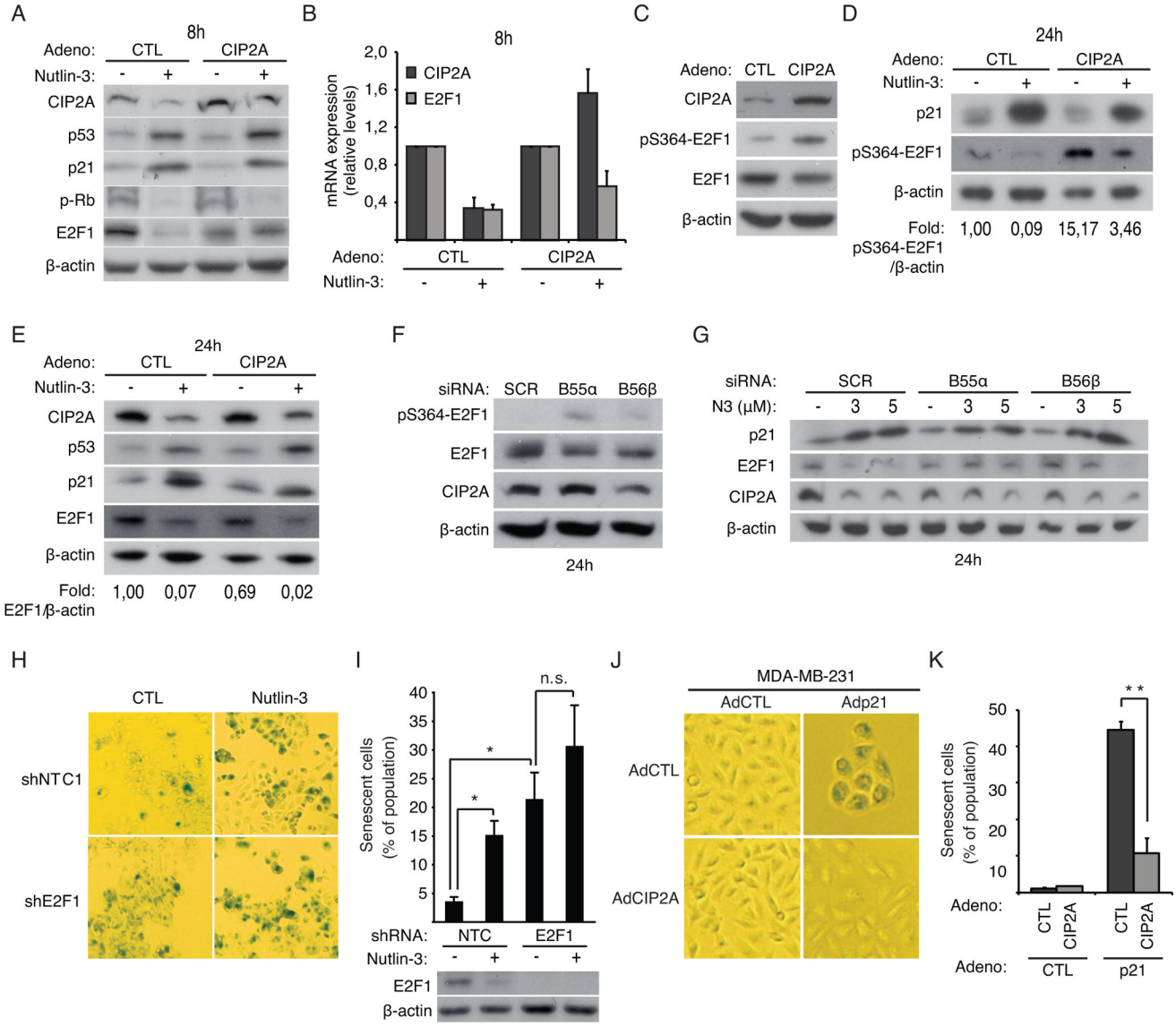

Figure 4. Positive feedback loop between CIP2A and E2F1 functions as a barrier for p21-mediated senescence induction

A) Western blot analysis of CIP2A, p53, p21, phosphorylated (Ser807/Ser811) Rb (ppRb) and E2F1 expression in either control (AdCTL) or CIP2A (AdCIP2A) adenovirus transduced (MOI=40) MCF-7 cells treated with Nutlin-3 (3μM) for 8 hours. Irrelevant data has been removed from the original graph. **B)** RT-PCR analysis of mRNA-expression of CIP2A and E2F1 from either control (AdCTL) or CIP2A (AdCIP2A) adenovirus transduced (MOI=40) MCF-7 cells (MOI=40) treated with Nutlin-3 (3μM) for 8 hours. Shown is mean +SEM of two independent experiments. **C)** Western blot analysis of pS364-E2F1, E2F1 and CIP2A expression in MCF-7 either control (AdCTL) or CIP2A (AdCIP2A) adenovirus transduced (MOI=40) MCF-7 cells. **D)** Western blot analysis of CIP2A, p21 and pS364-E2F1 expression in AdCTL or AdCIP2A transduced (MOI=40) MCF-7 cells treated with Nutlin-3 for 24 hours. **E)** Western blot analysis of p21, CIP2A and E2F1 expression in either control (AdCTL) or CIP2A (AdCIP2A) adenovirus transduced (MOI=40) MCF-7 cells treated with Nutlin-3 (3μM) for 24 hours. Irrelevant data has been removed from the

original graph. **F)** Western blot analysis of B55α, pS364-E2F1, E2F1 and CIP2A expression in either scrambled (SCR), B55α or B56β siRNA transfected MCF-7 cells. **G)** Western blot analysis of p21, E2F1 and CIP2A expression in either scrambled (SCR), B55α or B56β siRNA transfected MCF-7 cells treated with Nutlin-3 (3μM) for 24 hours. **H)** SA-beta-gal staining of either non-targeting shRNA (shNTC) or E2F1shRNA (shE2F1) stable expressing MCF-7 cells treated with Nutlin-3 (2μM) for 3 days. **I)** Percentage of SA-β-gal stained and morphologically flattened cells in either shNTC or shE2F1 expressing MCF-7 cells treated with Nutlin-3 (2μM) for 3 days. Shown is mean of replicates +SEM from one representative experiment. ** (shNTC control vs. shNTC N3) p=0,0019, ** (shNTC control vs. shE2F1 control) p=0,0032 and n.s. p=0,1358 by Student's t-test. **J)** SA-beta-gal staining of MDA-MB-231 cells 3 days after transduction with combination of indicated adeno viruses. AdCIP2A and AdCTL were transduced at MOI=80 and Adp21 and AdCTL at MOI=150. **K)** Percentage of SA-β-gal positive and morphologically flattened MDA-MB-231 cells 3 days after transduction with combination of indicated adenoviruses **(I)**. Shown is mean +SEM from a representative experiment. ** p=0,0021 by Student's t-test. **A,C,D,E,F,G,H,J)** Shown is a representative result of at least two independent experiments with similar results.

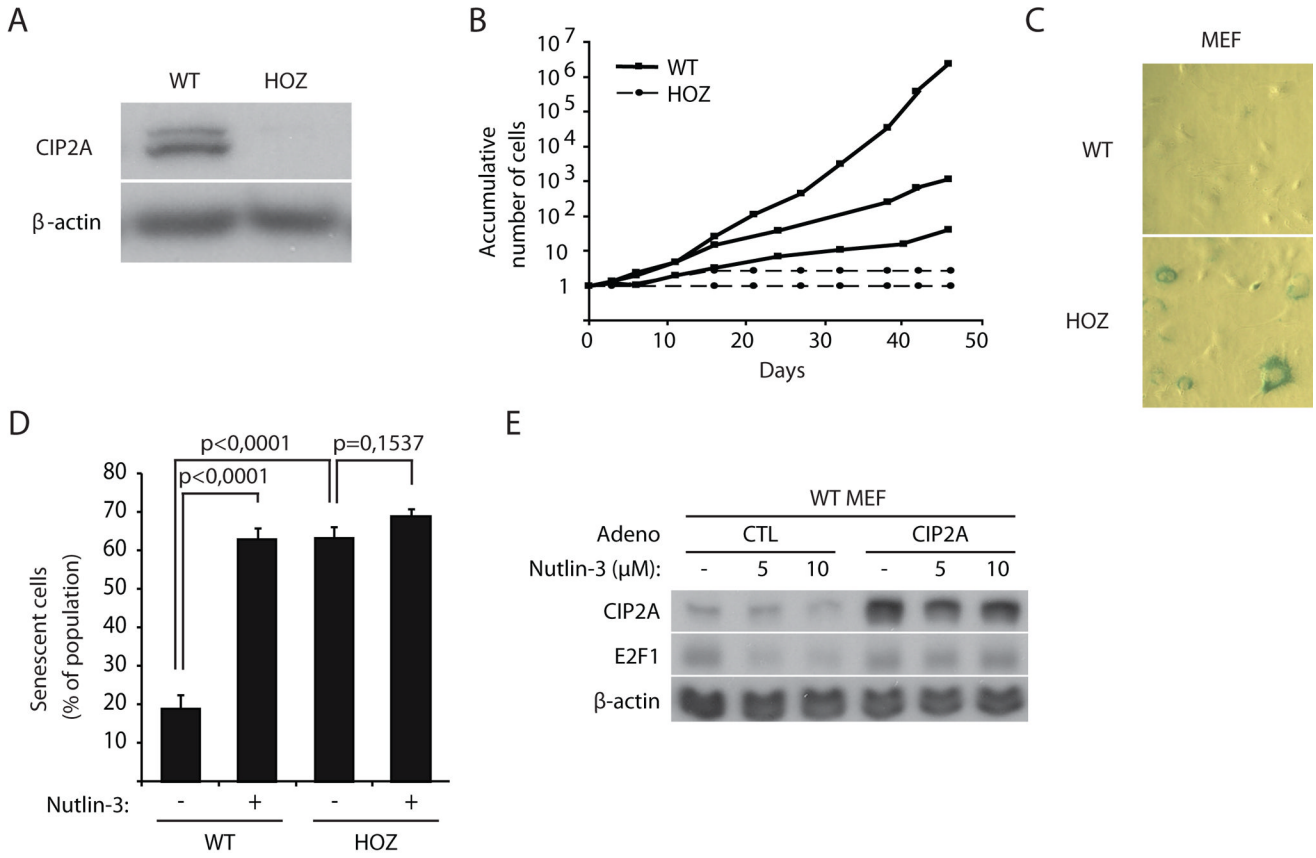

Figure 5. Inhibition of CIP2A inhibits growth and induces senescence in mouse embryonic fibroblasts

A) Western blot analysis of CIP2A expression in MEFs isolated from wild-type (WT) and CIP2A genetrap hypomorph (CIP2A^{HOZ}) mouse embryos. **B)** Growth curve presenting proliferation capacity of WT and CIP2A^{HOZ} MEFs. MEFs from 3 different WT or CIP2A^{HOZ} embryos were cultured for 46 days. Two CIP2A^{HOZ} MEF colonies ceased to proliferate after first passage and therefore their flat curves overlap in the graph. **C)** SA-beta-gal staining of wild-type (WT) and CIP2A^{HOZ} MEFs at passage 4. Shown is a representative of two independent experiments. **D)** Percentage of SA-β-gal stained WT and CIP2A^{HOZ} MEFs treated with Nutlin-3 (10μM) for 3 days. Shown is mean +SEM of two independent experiments. P values by Student's t-test. **E)** Western blot analysis of CIP2A and E2F1 expression in either control (AdCTL) or CIP2A (AdCIP2A) adenovirus transduced (MOI=50) wild-type MEFs. Shown is a representative result of two independent experiments.

Europe PMC Funders Author Manuscripts

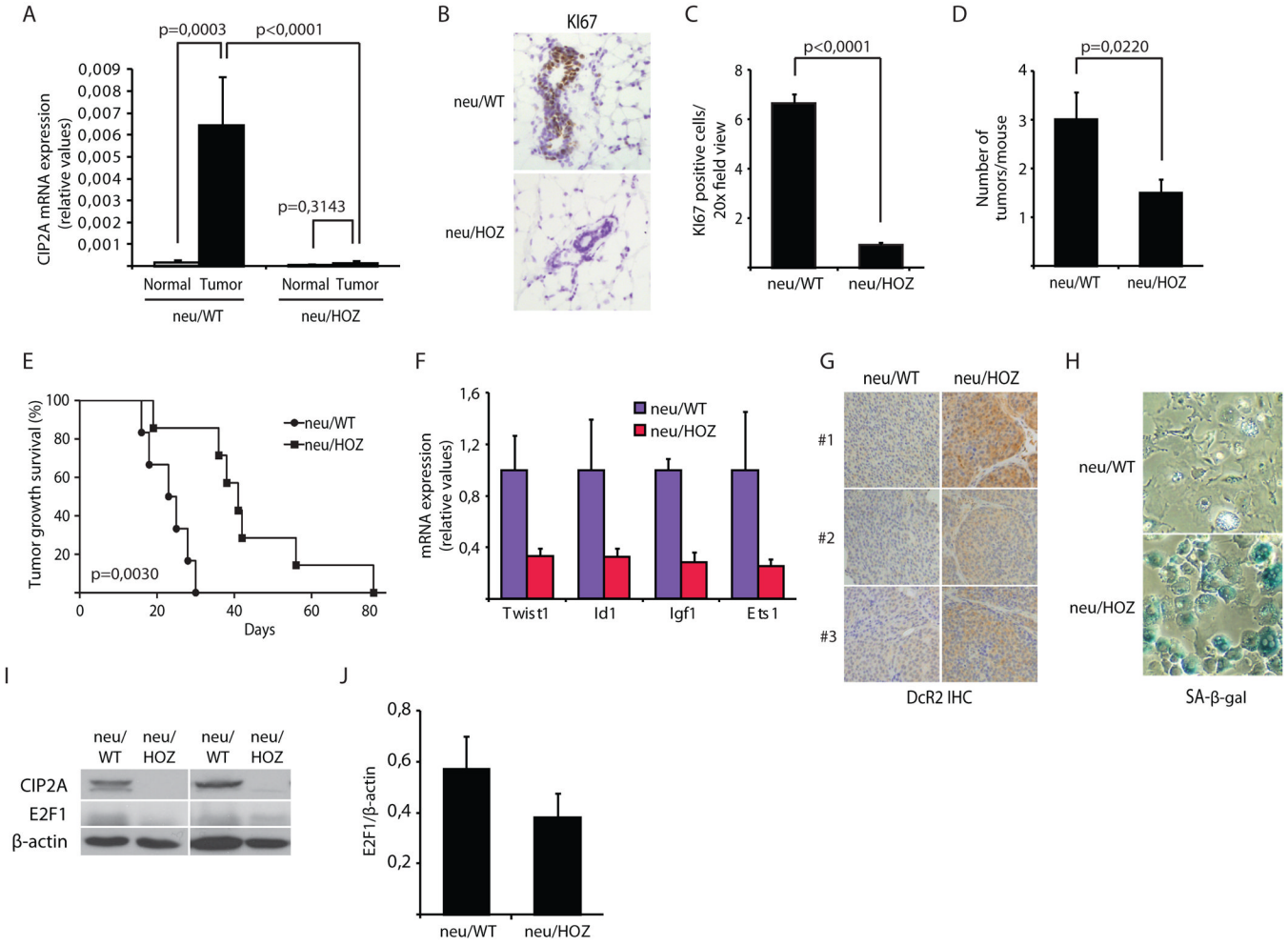

Figure 6. CIP2A inactivation induces senescence and growth arrest, and restricts tumorigenesis in a breast cancer mouse model

A) RT-PCR analysis of CIP2A mRNA expression from parental MMTVneu (neu/WT) and MMTVneu x CIP2A^{HOZ} (neu/HOZ) normal mammary glands and tumors. Shown is mean +SEM of mammary glands from 6 neu/WT and 8 neu/HOZ mice and 25 tumors from 9 neu/WT and 14 tumors from 10 neu/HOZ mice. P values by Mann-Whitney test. **B)** Representative Ki67 immunohistochemistry staining from 5 neu/WT and 4 neu/HOZ macroscopic tumor-free mouse mammary glands at the time of tumor appearance. **C)** Quantitation of Ki67 staining in **(B)**. Shown is mean +SEM of Ki67 positive cells in a field at 20x magnification. p<0,0001 by Mann-Whitney test. **D)** Number of mammary gland tumors per mouse in neu/WT and neu/HOZ mice. Tumors were counted when mice were sacrificed due to 20 mm size of the largest tumor. Shown is mean +SEM in 9 neu/WT and 10 neu/HOZ mouse. p=0,0220 by Student's t-test. **E)** Tumor growth was followed from the day of tumor appearance to the day when the mice had to be sacrificed due to 20 mm size of the largest tumor. Shown is tumor growth (days) of 6 neu/WT and 7 neu/HOZ mice. p=0,0030 by log-rank test. **F)** RT-PCR analysis of senescence markers from neu/WT and neu/HOZ mammary gland tumors at the time of tumor appearance. Shown is mean +SEM from two neu/WT and two neu/HOZ tumors.**G)** Representative DcR2 immunohistochemistry staining from 7 neu/WT and 3 neu/HOZ mammary gland tumors at the time of tumor appearance. **H)** Representative SA-beta-gal staining from isolated neu/WT

Europe PMC Funders Author Manuscripts

and neu/HOZ mammary gland tumor cells after 3 days in culture. Experiment was performed twice with cells isolated from 2 different neu/WT and 2 different neu/HOZ mammary gland tumors with similar results. **I)** Representative western blot analysis of CIP2A and E2F1 expression in neu/WT and neu/HOZ mammary gland tumors isolated at the time of tumor appearance. **J)** Quantitation of E2F1 protein levels from figure **(I)**. E2F1 protein expression normalized to β-actin. Shown is mean +SEM of 9 neu/WT and 6 neu/HOZ tumor lysates.

A

Variable	CIP2A immunostatus Neg. (-) (n = 186)	Weakly pos. (+) (n = 599)	Strongly pos. (++) (n = 99)	p-value
p53 expression (%)				
Neg-low	152 (24.3)	417 (66.7)	56 (9.0)	
High	25 (11.5)	154 (71.0)	38 (17.5)	<0.0001
Not available	9	28	5	
Tumor size (%)				
≤ 2 cm	96 (25.9)	242 (65.4)	32 (8.6)	
> 2 cm	90 (17.5)	357 (69.5)	67 (13.0)	0.0032
Tumor diameter (mm)				
Median (range)	20.0 (4-100)	23.0 (6-160)	25.0 (7-80)	0.011
Not available	3	10	0	
Histological grade (%)				
Grade 1 or 2	124 (26.2)	319 (67.4)	30 (6.3)	
Grade 3	53 (14.2)	253 (68.0)	66 (17.7)	<0.0001
Not available	9	27	3	
Ki-67 expression (%)				
Median (range)	15 (0-90)	25 (0-100)	40 (5-95)	<0.0001
Not available	20	63	10	

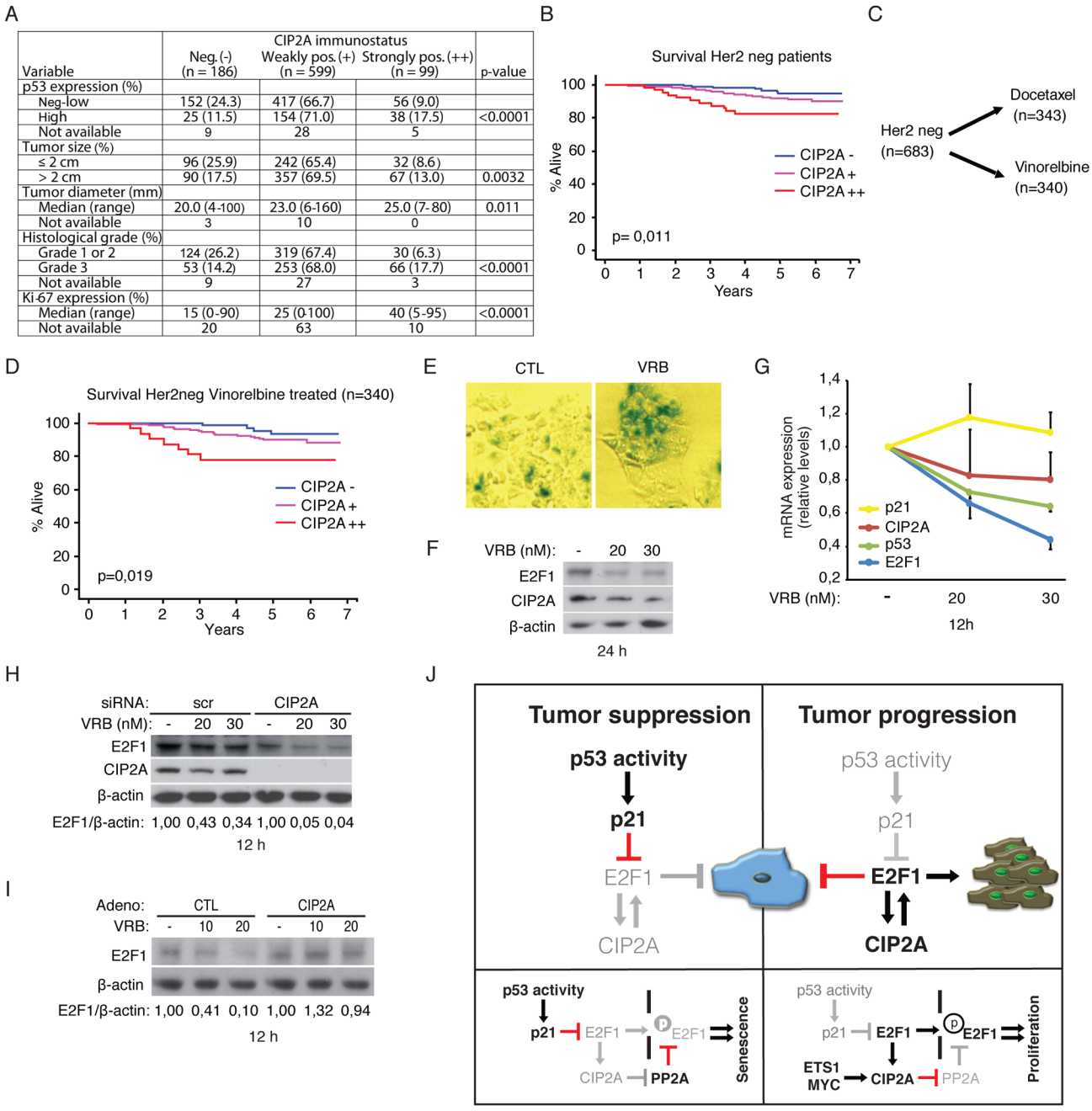

Figure 7. CIP2A confers resistance of human breast tumors to senescence-inducing chemotherapy

A) CIP2A expression in human breast cancer tumors in FinHer study. CIP2A is expressed in 79% of breast tumors and correlates with high p53 immunopositivity and with other poor prognostic factors. P values by chi-squared test, except for Ki-67 and tumor diameter Kruskal-Wallis test was used. **B)** CIP2A expression significantly correlates with survival of patients with HER2-negative tumors. CIP2A− = CIP2A negative tumor, CIP2A+ = moderately CIP2A positive tumor, CIP2A++ = high CIP2A expressing tumor. P=0,011 by log-rank test. **C)** Stratification scheme of patients with HER2-negative tumors to therapies including either vinorelbine followed by FEC (n=340) or docetaxel followed by FEC

(n=343). **D)** CIP2A overexpression significantly associates with poor survival of vinorelbine + FEC treated HER2-negative patients. P=0,019 by log-rank test. **E)** SA-beta-gal staining of MCF-7 cells treated with vinorelbine (VRB, 30nM) for 5 days. **F)** Western blot analysis of E2F1 and CIP2A expression in MCF-7 cells treated with vinorelbine (VRB, 20nM and 30nM) for 24 hours. **G)** RT-PCR analysis of p53, p21, E2F1 and CIP2A mRNA expression in MCF-7 cells treated with vinorelbine (VRB, 20nM and 30nM). Shown is mean +SEM of two independent experiments. **H)** Western blot analysis of E2F1 and CIP2A expression in either scrambled (SCR) or CIP2A siRNA transfected MCF-7 cells treated with vinorelbine (VRB, 20nM and 30nM) for 12 hours. Quantitation of E2F1 expression normalized to β-actin expression is shown below the graph. **I)** Western blot analysis of E2F1 in either control (AdCTL) or CIP2A (AdCIP2A) adenovirus transduced (MOI=40) MCF-7 cells treated with vinorelbine (VRB, 10nM and 20nM) for 12 hours. Quantitation of E2F1 expression normalized to β-actin expression is shown below the graph. **(E, F,H,I**) Shown is representative result of at least two experiments with identical results. **J)** Schematic presentation of the positive feedback loop between E2F1 and CIP2A in regulation of cellular senescence sensitivity downstream of p53. Inactive molecules and functions are shown in grey. In non-transformed cells (left panel), either oncogene-or chemotherapy-induced p53 activity inhibits E2F1 expression resulting in subsequent inhibition of CIP2A expression. CIP2A inhibition further inhibits E2F1 protein expression by post-translational mechanism involving PP2A. Loss of E2F1-CIP2A positive feedback activity provokes cellular senescence and hence tumor suppression. In tumorigenic cells (right panel) in which p53 activity is inhibited either by mutations or by enhanced proteolytic degradation, E2F1-CIP2A positive feedback loop is active, resulting in inhibition of senescence induction and hence tumor progression. Importantly, in addition to p53 inactivation, activity of CIP2A-E2F1 feedback may be stimulated by ETS1 and MYC that enhance CIP2A expression.